J. Phys. Chem. A **1998,** *102,* 10655−10670

Thermal Decomposition of 2,5-Dimethylfuran. Experimental Results and Computer Modeling

Assa Lifshitz,* Carmen Tamburu, and Ronen Shashua

Department of Physical Chemistry, The Hebrew University, Jerusalem 91904, Israel

Received: June 25, 1998; In Final Form: September 10, 1998

The thermal reactions of 2,5-dimethylfuran were studied behind reflected shock waves in a pressurized driver single pulse shock tube over the temperature range 1070−1370 K and overall densities of $\sim 3 \times 10^{-5}$ mol/cm^3. A large number of products resulting from unimolecular cleavage of the ring and consecutive free radical reactions were obtained under shock heating. A methyl group migration from C(2) to C(3) in the ring with the elimination of CO produces four isomers of C_5H_8 in unimolecular processes. An additional unimolecular process is the decomposition of 2,5-dimethylfuran to CH_3CO and C_4H_5 which is an important initiator of free radical reactions. Ejection of a hydrogen atom from the methyl group in the molecule is another channel for initiation of free radical reactions in the system. The 2,5-dimethylfuryl radical, which is obtained in the process of H-atom ejection, decomposes in channels similar to those of 2,5-dimethylfuran to produce, among other products, C_5H_7, which is the precursor of cyclopentadiene. The major decomposition product found in the post shock mixtures is carbon monoxide. The rate constant of its overall formation is estimated as $k_{CO} = 10^{15.81}\exp(-75.1 \times 10^3/RT)$ s^{-1} where R is expressed in units of cal/(K mol). Other products that were found in the postshock samples in decreasing order of abundance were C_4H_4, C_2H_2, and CH_4 in roughly the same abundance, C_2H_4, C_2H_6, $CH_2{=}CH{-}CH{=}CH_2$, cyclopentadiene p-C_3H_4, and a-C_3H_4 and 2-methylfuran. Other isomers of C_4H_6, C_5H_6 and C_5H_8, and some additional products were found in very small quantities. The total decomposition of 2,5-dimethylfuran in terms of a first-order rate constant is given by: $k_{total} = 10^{16.22}\exp(-77.5 \times 10^3/RT)$ s^{-1}. An oxygen−carbon mass balance among the decomposition products is obtained. A reaction scheme composed of 50 species and some 180 elementary reactions accounts for the product distribution over the temperature range covered in this study. First-order Arrhenius rate parameters for the formation of the various reaction products are given, a reaction scheme is suggested, and results of computer simulation and sensitivity analysis are shown. Differences and similarities among the reactions of furan, 2-methylfuran, and 2,5-dimethylfuran are discussed.

I. Introduction

We have recently published a detailed investigation on the thermal decomposition of 2-methylfuran in a single pulse shock tube,[1] covering the temperature range 1070−1370 K at total densities of $\sim 3 \times 10^{-5}$ mol/cm^3. A large number of products were obtained under shock heating. It was shown that the unimolecular decomposition follows two parallel channels. They are 1,2 hydrogen atom migration from C(5) to C(4) and a methyl group migration from C(2) to C(3) in the ring.

Each channel was then followed by two parallel modes of ring cleavage. In the first channel, breaking the O−C(2) and the C(4)−C(5) bonds in ring yields CO and different isomers of C_4H_6

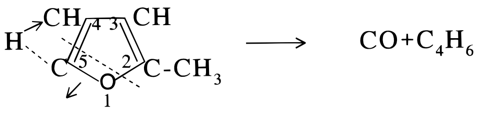

whereas breaking of the O−C(2) and the C(3)−C(4) bonds yields CH_2CO and two isomers C_3H_4

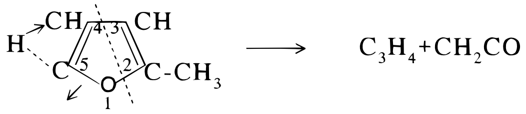

In the second channel, breaking the O−C(5) and the C(2)−C(3) bonds in the ring yields CO and 1-butyne

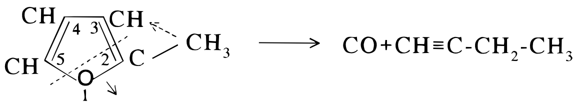

whereas in the second mode O−C(5), C(2)−C(3), and C(3)−C(4) are broken to yield CO, C_2H_2, and C_2H_4

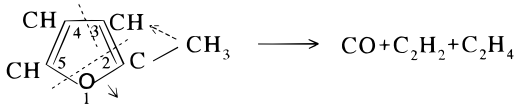

The four isomers of C_4H_6 were 1,3-butadiene, 1-butyne, 1,2-butadiene, and 2-butyne. The total decomposition of 2-methylfuran in terms of a first-order rate constant was found to be $k_{total} = 10^{16.22}\exp(-77.5 \times 10^3/RT)$ s^{-1}. A reaction scheme composed of 36 species and some 100 elementary reactions could account for the observed product distribution.[1]

We are not aware of another detailed study involving doubly substituted furans such as dimethylfuran. We are aware, however, of one VLPP study of 2,5-dimethylfuran[2] where only the overall decomposition rate was determined from which the high-pressure limit rate constant was evaluated.

10.1021/jp982772b CCC: $15.00

In this investigation we present data on the product distribution in shock heated mixtures of 2,5-dimethylfuran. A detailed mechanism is suggested, a reaction scheme which includes unimolecular decompositions, dissociative attachments, and free radical reactions is composed, and computer simulation is performed.

II. Experimental Section

1. Apparatus. The thermal reactions of 2,5-dimethylfuran were studied behind reflected shocks in a pressurized driver, 52 mm i.d. single-pulse shock tube. The tube and its mode of operation have been described in an earlier publication[3] and will be given here only very briefly.

The driven section was 4 m long and the driver had a variable length up to a maximum of 2.7 m. It could be varied in small steps in order to tune for the best cooling conditions. A 36 L dump tank was connected to the driven section at 45° angle near the diaphragm holder in order to prevent reheating by reflection of transmitted waves. The driven section was separated from the driver by a Mylar polyester film of various thickness depending upon the desired shock strength.

Before each test the tube was pumped down to approximately 3×10^{-5} Torr. After performing an experiment, gas samples were collected from the tube through an outlet in the driven section (near the end plate) in 150 cm^3 glass bulbs and were then analyzed on a Carlo-Erba Model VEGA-2000 gas chromatograph using a flame ionization detector. Reflected shock temperatures were calculated from the extent of decomposition of 1,1,1-trifluoroethane which was added in small quantities to the reaction mixture and served as an internal standard. Its decomposition to $CH_2{=}CF_2{+}HF$ is a first-order unimolecular reaction which under the temperature and pressure conditions of this investigation has a rate constant of[4] $k_{first} = 10^{14.8}\exp(-74.0 \times 10^3/RT)$ s^{-1}. Reflected shock temperatures were calculated from the relation:

$$T = -(E/R)/\left[\ln\left\{-\frac{1}{At}\ln(1-\chi)\right\}\right] \quad \text{(I)}$$

where t is the reaction dwell time and χ is the extent of decomposition defined as

$$\chi = [CH_2{=}CF_2]_t/([CH_2{=}CF_2]_t + [CH_3CF_3]_t)$$

The additional reflected shock parameters were calculated from the measured incident shock velocities using the three conservation equations and the ideal gas equation of state. Dwell times of approximately 2 ms were measured with an accuracy of ±5%. Cooling rates were approximately 5×10^5 K/s.

2. Materials and Analysis. Reaction mixtures containing 0.5% 2,5-dimethylfuran and 0.1% 1,1,1-trifluoroethane in argon were prepared manometrically and stored in 12 L glass bulbs at 700 Torr. Both the bulbs and the line were pumped down to $\sim 10^{-5}$ Torr before the preparation of the mixtures. 2,5-dimethylfuran was obtained from Aldrich Chemical Co. and showed only one GC peak. The argon used was Matheson ultrahigh purity grade, listed as 99.9995%, and the helium was Matheson pure grade listed as 99.999%. All the materials were used without further purification.

The gas chromatographic analyses of the postshock mixtures were performed on two columns with flame ionization detectors. The analyses of all the products except for CO were performed on a 2 m Porapak N column. Its initial temperature of 35 °C was gradually elevated to 190 °C in an analysis which lasted about 50 min. A typical chromatogram of 0.5% 2,5-dimethylfuran in argon shock heated to 1238 K is shown in Figure 1.

Carbon monoxide was analyzed on a 2 m molecular sieve 5 Å column at 35 °C. It was reduced at 400 °C to methane prior to its detection using a Chrompak methanyzer with a carrier gas composed of 50% hydrogen and 50% argon. These analyses gave the ratio $[CO]/[CH_4]$. From these ratios and the known methane concentration obtained in the Porapak N analyses, the concentration of CO could be calculated for each run. The ratio $[CO]/[CH_4]$ in a standard mixture of methane and carbon monoxide was determined periodically in order to verify a complete conversion of the latter to methane in the methanyzer.

In the course of analyzing the raw data we encountered some separation problems which were solved by using the SIM mode of a Hewlett-Packard model 5970 mass selective detector connected to a Hewlett-Packard model 5890 gas chromatograph. The peaks of 1-butyne and 1,2-butadiene were hidden under a large peak of C_4H_4. Two peaks of C_5H_8 were hidden under a larger peak of cyclopentadiene. The procedure of determining the magnitude of the hidden peaks is described in detail in the article on the decomposition of 2-methylfuran.[1]

We have carried out also a separate series of experiments in order to verify the presence or absence of ketene and/or methyl ketene in the postshock mixtures. Methylketene can be formed by a unimolecular decomposition of 2,5-dimethylfuran. Ketene and methyl ketene tend to react with small quantities of water absorbed in various location on the way to the GC and produce acetic and propionic acids which are also absorbed and hard to analyze. The postshock mixtures in this series of experiments were collected in bulbs containing small quantities of methyl alcohol. In this way, methyl acetate is formed from ketene and methyl propionate from methyl ketene. The latter can be, at least qualitatively, analyzed. We did not identify any methyl propionate in the post shock mixtures and only traces of methyl acetate

The concentrations of the reaction products $C_5(\mathrm{pr})_i$ were calculated from their GC peak areas from the following relations:[5]

$$C_5(\mathrm{pr})_i = A(\mathrm{pr}_i)_t/S(\mathrm{pr}_i)(C_5(\text{2,5-dimethylfuran})_0/A(\text{2,5-dimethylfuran})_0) \quad \text{(II)}$$

$$C_5(\text{2,5-dimethylfuran})_0 = p_1\%(\text{2,5-dimethylfuran})(\rho_5/\rho_1)/100RT_1 \quad \text{(III)}$$

$$A(\text{2,5-dimethylfuran})_0 = A(\text{2,5-dimethylfuran})_t + 1/6\Sigma N(\mathrm{pr}_i)\times A(\mathrm{pr}_i)_t/S(\mathrm{pr}_i) \quad \text{(IV)}$$

In these relations $C_5(\text{2,5-dimethylfuran})_0$ is the concentration of 2,5-dimethylfuran behind the reflected shock prior to decomposition, and $A(\text{2,5-dimethylfuran})_0$ is the calculated GC peak area of 2,5-dimethylfuran prior to decomposition (eq IV) where $A(\mathrm{pr}_i)_t$ is the peak area of a product i in the shocked sample. $S(\mathrm{pr}_i)$ is its sensitivity relative to 2,5-dimethylfuran, and $N(\mathrm{pr}_i)$ is the number of its carbon atoms. ρ_5/ρ_1 is the compression behind the reflected shock, and T_1 is the temperature of the shock tube.

The identification of the reaction products was based on their GC retention times but was also assisted by a Hewlett-Packard model 5970 mass selective detector. The sensitivities of the various products to the FID were determined relative to 2,5-dimethylfuran from standard mixtures. The areas under the GC peaks were integrated with a Spectra Physics Model SP4200

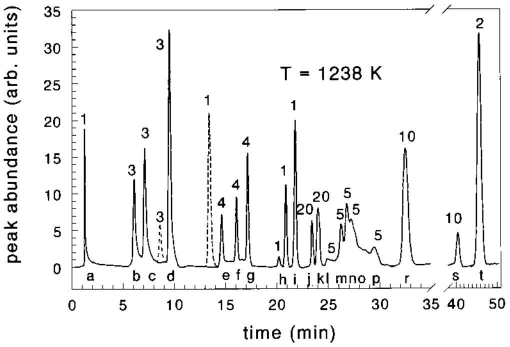

Figure 1. Gas chromatogram of a post-shock mixture of 0.5% 2,5-dimethylfuran in argon heated to 1238 K. The numbers on the peaks are multiplication factors. The measured peak heights are lower than those on the figure by these factors. (a) CH_4, (b) C_2H_4, (c) C_2H_6, (d) C_2H_2, (e) C_3H_6, (f) allene, (g) propyne, (h) 1,3-butadiene, (i) C_4H_4, 1,2-butadiene, 1-butyne, (j) 2-butyne, (k) C_4H_2, (l) furan, 1,4-pentadiene, (m) 1,2-pentadiene, (n) cyclopentadiene, (o) 1,3-pentadiene, (p) 1,2,4-pentatriene, 2-pentyne, (r) 2-methylfuran, (s) C_6H_6, (t) 2,5-dimethylfuran.

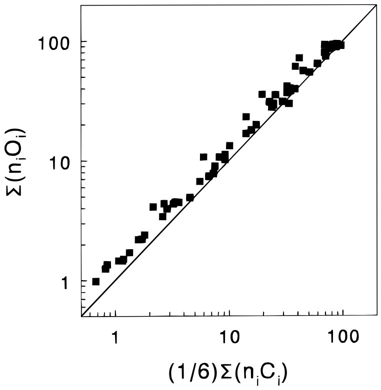

Figure 2. Oxygen−carbon mass balance among the decomposition products. The 45° line represent a perfect carbon−oxygen mass balance.

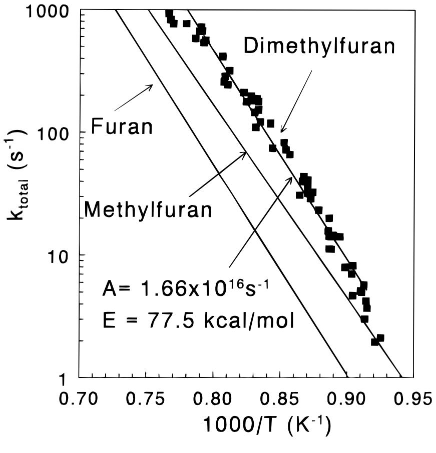

Figure 3. Arrhenius plot of the first-order rate constant for the overall decomposition of 2,5-dimethylfuran. The rate constant is calculated from the relation: $k_{total} = \ln\{[2,5\text{-dimethylfuran}]_t/[2,5\text{-dimethylfuran}]_0\}/t$. The value obtained is: $k_{total} = 10^{16.22}\exp(-77.5 \times 10^3/RT)$ s^{-1}. The total decomposition of 2-methylfuran and furan is also shown for comparison.

computing integrator and were transferred after each analysis to a PC for data reduction and graphical presentation.

III. Results

To determine the distribution of reaction products, some 70 tests were run with mixtures containing 0.5% 2,5-dimethylfuran in argon, covering the temperature range 1070−1370 K. Extents of pyrolysis as low as a few hundredths of one percent were determined. Details of the experimental conditions and the distribution of reaction products are given in Table 1. The percent of a given product in the total sample, as shown in the table, corresponds to its mole fraction in the postshock mixture irrespective of the number of its carbon atoms.

The balance of oxygen vs carbon among the decomposition products is shown in Figure 2. The concentrations of carbon monoxide and methylfuran are plotted against one-sixth the sum of the concentrations of all the decomposition products (including carbon monoxide and methylfuran) each multiplied by the number of its carbon atoms. One-sixth is the ratio of oxygen to carbon in the reactant molecule. The 45° line in the figure represents a complete mass balance. As can be seen, there is no major deviation from an oxygen−carbon balance over the temperature range of the investigation.

Figure 3 shows the rate constant for the total decompositions of 2,5-dimethylfuran, calculated as a first-order rate constant from the relation:

$$k_{total} = -\ln\{[2,5\text{-dimethylfuran}]_t/[2,5\text{-dimethylfuran}]_0\}/t \quad \text{(V)}$$

The value obtained is $k_{total} = 10^{15.43}\exp(-73.1 \times 10^3/RT)$ s^{-1} where R is expressed in units of cal/(K mol). The rate constants for the total decompositions of furan and 2-methylfuran are also shown for comparison. As can be seen, the total decomposition of 2,5-dimethylfuran is higher than that of 2-methylfuran which is already higher than that of furan. Figures 4−6 show three examples of Arrhenius plots of the first-order production rates of CO, C_2H_2, and 1,3-butadiene calculated from the relation

$$k_{product} = \frac{[\text{product}]_t}{[\text{reactant}]_0 - [\text{reactant}]_t} k_{total} \quad \text{(VI)}$$

Values of E obtained from the slopes of such lines for the reaction products and their corresponding preexponential factors are summarized in Table 2. It should be mentioned that the parameters for the product formation do not represent elementary unimolecular reactions owing to further decompositions and involvement of free radical reactions. This presentation simply provides a convenient way to summarize general rates.

IV. Discussion

1. Unimolecular Processes; Production of Stable Products. We have recently demonstrated, in the study on the decomposition of 2-methylfuran,[1] that the latter undergoes a number of unimolecular decomposition channels to produce both stable molecules (C_4H_6 isomers and CO) and unstable intermediates which are responsible for the propagation of free radical reactions. The major unimolecular channel in the decomposition of 2-methylfuran is a 1,2-H-atom migration from C(5) to C(4) in the ring, followed by elimination of carbon monoxide and formation of several C_4H_6 isomers

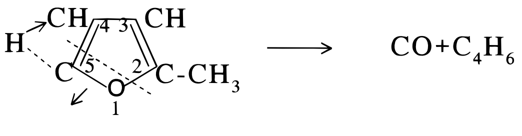

and to a much lesser extent a migration of the CH_3 group from

TABLE 1: Experimental Conditions and Product Distribution in Percent

T_5 (K)	$C_5 \times 10^5$ (mol/cm^3)	t (ms)	dimethyl-furan	1,3-butadiene	1,2-butadiene	1-butyne	2-butyne	C_4H_4	C_4H_2	cyclo-pentadiene	1,2,4-pentatriene	1,3-penta-diene	1,2-pentadiene
1081	2.97	2.00	98.61	8.93×10^{-2}	1.38×10^{-3}	1.63×10^{-2}		3.37×10^{-2}					
1086	3.19	2.15	98.70	0.115	2.00×10^{-3}	2.15×10^{-2}		6.00×10^{-2}		7.93×10^{-2}	0.0021	2.16×10^{-2}	1.35×10^{-2}
1093	3.02	2.10	97.63	0.187	3.67×10^{-3}	3.60×10^{-2}		0.115				9.78×10^{-3}	6.12×10^{-3}
1094	2.76	2.00	97.63	0.130	2.60×10^{-3}	2.52×10^{-2}		3.83×10^{-2}		0.156	0.0046	4.50×10^{-2}	2.81×10^{-2}
1095	3.17	2.20	97.92	0.179	3.66×10^{-3}	3.48×10^{-2}		9.93×10^{-2}		0.113	0.003	2.95×10^{-2}	1.85×10^{-2}
1096	2.15	2.20	96.73	0.245	5.05×10^{-3}	4.77×10^{-2}	1.75×10^{-3}	0.176		0.122	0.0032	3.15×10^{-2}	2.00×10^{-2}
1098	3.15	2.20	97.26	0.200	4.31×10^{-3}	3.92×10^{-2}		0.149		0.101	0.0027	2.59×10^{-2}	1.63×10^{-2}
1099	2.94	2.15	97.12	0.215	4.73×10^{-3}	4.24×10^{-2}		0.224		0.126	0.0033	3.23×10^{-2}	2.03×10^{-2}
1106	3.07	2.25	96.80	0.272	6.82×10^{-3}	5.52×10^{-2}		0.232		0.162	0.0042	4.00×10^{-2}	2.52×10^{-2}
1106	2.86	1.94	95.87	0.265	6.52×10^{-3}	5.34×10^{-2}	8.1×10^{-4}	0.219		0.207	0.0059	5.63×10^{-2}	3.55×10^{-2}
1107	3.02	2.30	95.90	0.293	7.44×10^{-3}	5.94×10^{-2}		0.262		0.165	0.0043	4.06×10^{-2}	2.56×10^{-2}
1113	3.01	2.15	95.56	0.314	8.91×10^{-3}	6.55×10^{-2}		0.268		0.185	0.0048	4.43×10^{-2}	2.81×10^{-2}
1118	2.98	2.20	91.78	0.610	1.88×10^{-2}	0.129		0.593		0.300	0.0077	7.01×10^{-2}	4.45×10^{-2}
1124	3.01	2.25	91.58	0.592	2.01×10^{-2}	0.128		0.586		0.356	0.0091	8.12×10^{-2}	5.18×10^{-2}
1125	2.79	2.00	91.99	0.486	1.68×10^{-2}	0.105	2.34×10^{-3}	0.434		0.291	0.0081	7.14×10^{-2}	4.56×10^{-2}
1126	2.15	2.25	91.57	0.647	2.27×10^{-2}	0.141		0.630		0.173	0.0044	3.91×10^{-2}	
1126	2.96	1.92	93.39	0.402	1.41×10^{-2}	8.80×10^{-2}	2.00×10^{-3}	0.356					
1128	2.79	1.88	91.99	0.618	2.24×10^{-2}	0.136		0.422					
1128	2.77	2.20	89.68	0.807	2.92×10^{-2}	0.177	8.72×10^{-3}	1.050		0.624	0.0159	0.140	8.95×10^{-2}
1128	3.01	2.30	92.65	0.585	2.12×10^{-2}	0.128		0.630		0.415	0.0106	9.32×10^{-2}	5.96×10^{-2}
1129	2.87	2.20	91.24	0.664	2.44×10^{-2}	0.146		0.708		0.436	0.0111	9.74×10^{-2}	6.23×10^{-2}
1138	2.90	2.30	87.58	0.863	3.62×10^{-2}	0.195		1.003		0.693	0.0177	0.149	9.60×10^{-2}
1144	2.15	2.20	85.65	1.500	6.82×10^{-2}	0.344	1.45×10^{-2}	1.734		0.951	0.0243	0.200	0.129
1146	2.53	2.25	85.13	1.104	5.17×10^{-2}	0.255	4.77×10^{-3}	1.490	1.20×10^{-2}	0.915	0.0234	0.190	0.123
1149	2.84	2.30	83.36	1.148	5.59×10^{-2}	0.267	6.81×10^{-3}	1.453		0.953	0.0244	0.196	0.127
1149	2.92	2.25	80.81	1.348	6.57×10^{-2}	0.314	4.67×10^{-3}	1.614		0.911	0.0233	0.187	0.121
1149	2.45	2.25	79.07	1.514	7.37×10^{-2}	0.353		2.000		1.106	0.0283	0.227	0.148
1153	2.80	2.30	76.91	1.532	7.85×10^{-2}	0.360	8.52×10^{-3}	1.901		1.015	0.0261	0.205	0.134
1154	2.15	2.30	79.66	1.536	7.96×10^{-2}	0.362	1.37×10^{-2}	1.866		1.091	0.0281	0.220	0.143
1157	2.73	1.96	82.92	0.961	5.17×10^{-2}	0.228	0.0087	1.227					
1167	2.71	2.20	70.22	2.064	0.124	0.501	1.47×10^{-2}	3.014	2.79×10^{-2}	0.680	0.0439	0.322	0.212
1171	2.72	2.25	67.96	2.209	0.139	0.536	1.84×10^{-2}	3.162	3.64×10^{-2}	1.873	0.0493	0.353	0.234
1173	2.65	2.20	65.26	2.374	0.152	0.583	2.08×10^{-2}	3.407	1.41×10^{-2}	2.120	0.0560	0.397	0.263
1185	2.64	2.02	67.56	1.656	0.119	0.415	2.38×10^{-2}	2.170		1.355	0.0389	0.256	0.172
1187	2.86	2.25	54.01	3.001	0.219	0.754	3.35×10^{-2}	4.366		2.586	0.0704	0.460	0.309
1187	2.52	2.20	55.73	2.887	0.210	0.725	3.45×10^{-2}	4.347	3.46×10^{-2}	2.610	0.0711	0.464	0.312
1187	2.72	2.30	54.35	2.955	0.215	0.742	3.77×10^{-2}	4.515	3.14×10^{-2}	2.654	0.0723	0.472	0.318
1198	2.57	2.08	54.71	2.283	0.181	0.581	4.17×10^{-2}	3.706	4.40×10^{-2}	2.453	0.0724	0.441	0.300
1200	2.15	2.20	48.65	3.414	0.275	0.871	5.70×10^{-2}	5.277	7.72×10^{-2}	3.125	0.0883	0.531	0.362
1200	2.15	2.20	45.02	3.982	0.320	1.016	5.92×10^{-2}	6.223	7.60×10^{-2}	3.460	0.0977	0.588	0.401
1202	2.68	2.15	42.32	3.728	0.304	0.953	4.79×10^{-2}	5.994		3.168	0.0901	0.535	0.366
1203	3.16	1.94	55.64	2.300	0.188	0.588	4.56×10^{-2}	3.590	4.95×10^{-2}				
1204	2.49	2.00	50.07	2.447	0.202	0.626	3.55×10^{-2}	4.095	5.07×10^{-2}	2.446	0.0735	0.429	0.294
1206	2.46	2.25	42.44	3.754	0.314	0.963	6.11×10^{-2}	6.083	9.17×10^{-2}	3.424	0.0986	0.571	0.392
1208	2.68	1.96	44.76	3.177	0.269	0.818	7.87×10^{-2}	4.744	5.30×10^{-2}	4.022	0.122	0.726	0.480
1213	2.59	2.16	43.46	2.657	0.632	2.500	5.41×10^{-2}	4.458	0.330	2.952	0.0912	0.501	0.348
1216	2.55	2.15	39.96	3.906	0.345	1.010	7.35×10^{-2}	6.468	0.121	3.808	0.114	0.614	0.427
1232	2.44	2.15	27.51	4.514	0.424	1.171	9.40×10^{-2}	7.608	0.195	4.203	0.135	0.645	0.458
1234	2.19	1.94	37.17	3.378	0.319	0.876	9.04×10^{-2}	6.200	0.105	3.547	0.119	0.559	0.400
1237	2.92	2.04	30.48	3.581	0.341	0.927	8.87×10^{-2}	6.145	0.156	3.752	0.127	0.586	0.420

TABLE 1: (Continued)

T_5 (K)	$C_5 \times 10^5$ (mol/cm^3)	t (ms)	dimethyl-furan	1,3-butadiene	1,2-butadiene	1-butyne	2-butyne	C_4H_4	C_4H_2	cyclo-pentadiene	1,2,4-pentatriene	1,3-penta-diene	1,2-pentadiene
1238	2.34	2.04	30.10	3.228	0.309	0.838	7.75×10^{-2}	5.731	0.152				
1240	2.26	2.10	21.04	4.773	0.458	1.238	0.105	8.280	0.255	4.240	0.141	0.636	0.456
1260	2.29	2.10	13.97	4.967	0.484	1.276	0.118	8.870	0.363	4.136	0.154	0.587	0.433
1262	2.40	2.10	14.29	4.592	0.447	1.177	0.112	7.870	0.313	3.592	0.135	0.507	0.375
1264	2.16	2.10	10.07	4.767	0.463	1.220	0.105	8.620	0.373	3.481	0.133	0.489	0.363
1265	2.24	2.05	9.50	5.073	0.492	1.300	0.112	9.033	0.400	3.861	0.148	0.541	0.402
1267	2.29	2.10	10.35	4.840	0.469	1.235	0.119	8.643	0.395	3.840	0.151	0.535	0.400
1272	2.32	2.00	13.23	3.655	0.351	0.926	0.101	7.200	0.319	3.512	0.144	0.492	0.370
1283	2.18	2.00	8.72	4.474	0.418	1.120	0.108	8.994	0.530	3.323	0.144	0.445	0.341
1299	2.65	2.14	7.44	3.549	0.311	0.864	9.83×10^{-2}	7.740	0.553	3.025		0.393	
1303	3.25	2.13	6.27	3.067	0.263	0.741	8.51×10^{-2}	7.050	0.652	2.660	0.135	0.343	0.270
1305	2.88	2.14	5.25	4.013	0.340	0.961	0.125	9.509	0.719	3.227	0.166	0.413	0.328
1311	2.07	1.85	3.99	3.902	0.319	0.925	9.42×10^{-2}	8.650	0.746	2.547	0.137	0.321	0.258
1314	3.23	1.98	4.21	3.356	0.269	0.791	9.02×10^{-2}	8.018	0.725	2.492	0.138	0.312	0.252
1324	3.34	2.04	4.15	2.463	0.176	0.542	6.88×10^{-2}	6.388	0.800	1.878	0.113	0.230	0.190
1342	2.63	2.08	2.79	2.080	0.131	0.452	7.24×10^{-2}	6.809	1.314	1.461	0.104	0.172	0.146
1344	1.90	1.90	2.66	2.010	0.124	0.434	3.91×10^{-2}	6.162	1.011	0.900	0.0658	0.107	9.14×10^{-2}
1350	2.58	2.16	1.72	1.686	9.80×10^{-2}	0.356	6.47×10^{-2}	5.230	1.495	0.960	0.073	0.111	9.64×10^{-2}
1352	1.82	1.80	3.01	2.296	0.130	0.482	5.39×10^{-2}	7.040	1.224	1.020	0.0811	0.120	0.104

T_5 (K)	$C_5 \times 10^5$	t (ms)	CO	CH_4	C_2H_4	C_2H_6	C_2H_2	C_3H_6	allene	propyne	methylfuran	C_6H_6
1081	2.97	2.00	0.745	0.296	2.16×10^{-2}	2.06×10^{-2}	3.90×10^{-2}			1.34×10^{-2}	0.118	
1086	3.19	2.15	0.578	0.298	1.64×10^{-2}	2.09×10^{-2}	5.80×10^{-2}		2.08×10^{-3}	1.46×10^{-2}		
1093	3.02	2.10	1.002	0.610	3.01×10^{-2}	5.27×10^{-2}	6.39×10^{-2}			1.94×10^{-2}	0.231	
1094	2.76	2.00	1.178	0.365	3.40×10^{-2}	8.56×10^{-2}	7.41×10^{-2}	1.27×10^{-2}		3.08×10^{-2}	0.163	
1095	3.17	2.20	0.969	0.434	2.74×10^{-2}	5.38×10^{-2}	8.34×10^{-2}		5.74×10^{-3}	2.66×10^{-2}		
1096	2.15	2.20	1.262	0.681	4.28×10^{-2}	6.11×10^{-2}	0.108		1.16×10^{-2}	3.25×10^{-2}	0.415	
1098	3.15	2.20	1.054	0.533	2.75×10^{-2}	4.18×10^{-2}	8.15×10^{-2}		7.64×10^{-3}	2.50×10^{-2}	0.431	
1099	2.94	2.15	1.151	0.552	2.90×10^{-2}	6.01×10^{-2}	0.103		9.77×10^{-3}	2.98×10^{-2}	0.279	
1106	2.86	1.94	1.785	0.738	5.00×10^{-2}	0.104	0.141	4.00×10^{-2}		6.37×10^{-2}	0.360	
1106	3.07	2.25	1.426	0.678	4.19×10^{-2}	7.72×10^{-2}	0.131		1.21×10^{-2}	3.97×10^{-2}		
1107	3.02	2.30	1.633	0.783	4.09×10^{-2}	7.34×10^{-2}	0.132		1.38×10^{-2}	3.87×10^{-2}	0.532	
1113	3.01	2.15	1.807	0.879	4.44×10^{-2}	7.24×10^{-2}	0.138		1.56×10^{-2}	4.32×10^{-2}	0.521	
1118	2.98	2.20	3.462	1.616	8.57×10^{-2}	0.227	0.276		3.07×10^{-2}	8.08×10^{-2}	0.671	
1124	3.01	2.25	3.489	1.650	9.07×10^{-2}	0.170	0.279		3.26×10^{-2}	8.60×10^{-2}	0.799	
1125	2.79	2.00	3.316	1.900	0.112	0.285	0.336	4.23×10^{-2}	4.03×10^{-2}	7.94×10^{-2}	0.439	
1126	2.15	2.25	3.417	1.656	0.133	0.308	0.294		5.00×10^{-2}	8.78×10^{-2}	0.824	
1126	2.96	1.92	3.481	1.207	8.29×10^{-2}	0.187	0.226	2.94×10^{-2}	2.57×10^{-2}	6.08×10^{-2}	0.451	
1128	2.77	2.20	3.834	1.820	0.113	0.277	0.368		5.17×10^{-2}	0.123	0.795	
1128	3.01	2.30	3.253	1.410	9.52×10^{-2}	0.200	0.290		5.85×10^{-2}	0.100		
1128	2.79	1.88	3.687	1.713	0.145	0.311	0.336	4.09×10^{-2}	4.00×10^{-2}	8.06×10^{-2}	0.462	
1129	2.87	2.20	3.542	1.614	9.25×10^{-2}	0.229	0.301		3.68×10^{-2}	9.22×10^{-2}	0.701	
1138	2.90	2.30	4.890	2.120	0.134	0.293	0.448		5.22×10^{-2}	0.129	1.307	
1144	2.15	2.20	5.853		0.300	0.759	0.821		0.111	0.231	1.314	
1146	2.53	2.25	5.694	2.503	0.171	0.488	0.553		7.34×10^{-2}	0.167	1.049	
1149	2.45	2.25	8.562	3.592	0.260	0.743	0.802		9.98×10^{-2}	0.234	1.188	
1149	2.92	2.25	8.124	3.412	0.253	0.507	0.713		9.13×10^{-2}	0.209	1.295	
1149	2.84	2.30	6.609	2.760	0.200	0.450	0.650		7.80×10^{-2}	0.182	1.477	
1153	2.80	2.30	9.866	4.025	0.303	0.621	0.867	0.296	0.115	0.260	1.478	
1154	2.15	2.30	7.556	3.702	0.336	0.806	0.864		0.121	0.241	1.375	

TABLE 1: Continued

T_5 (K)	$C_5 \times 10^5$	*t* (ms)	CO	CH_4	C_2H_4	C_2H_6	C_2H_2	C_3H_6	allene	propyne	methylfuran	C_6H_6
1157	2.73	1.96	8.657	2.894	0.312	0.758	0.792	9.31×10^{-2}	8.62×10^{-2}	0.215	0.796	
1167	2.71	2.20	12.22	4.644	0.420	1.158	1.255		0.175	0.347	1.457	9.86×10^{-2}
1171	2.72	2.25	12.84	4.940	0.458	1.087	1.374	0.370	0.218	0.384	1.650	0.105
1173	2.65	2.20	13.93	5.400	0.510	1.162	1.462	0.413	0.233	0.410	1.706	0.130
1185	2.64	2.02	16.94	3.004	0.627	1.966	1.330	0.236	0.266	0.370	1.343	0.153
1187	2.72	2.30	18.66	6.765	0.825	1.537	2.262	0.494	0.340	0.597	2.164	
1187	2.52	2.20	18.04	6.392	0.797	1.548	2.202	0.464	0.332	0.586	2.217	
1187	2.86	2.25	19.29	6.991	0.850	1.523	2.134	0.486	0.345	0.590	1.984	
1198	2.57	2.08	20.48	6.161	0.991	2.184	2.552	0.280	0.343	0.576	1.406	0.220
1200	2.15	2.20	17.88	8.804	1.437	2.641	3.485	0.674	0.555	0.873	2.100	0.309
1200	2.15	2.20	19.33	7.481	1.260	2.087	3.040	0.573	0.472	0.775	1.928	0.328
1202	2.68	2.15	23.72	7.924	1.138	2.555	3.008	0.647	0.496	0.792	1.958	0.256
1203	3.16	1.94	23.25	6.388	1.000	1.868	2.450	0.296	0.343	0.563	1.454	
1204	2.49	2.00	22.41	7.442	1.203	2.360	2.924	0.307	0.390	0.637	1.373	0.188
1206	2.46	2.25	22.66	7.954	1.265	2.372	3.281	0.623	0.536	0.842	1.975	0.300
1208	2.68	1.96	22.37	5.820	1.464	4.076	2.921	0.457	0.591	0.872	1.952	0.235
1213	2.59	2.16	25.27	6.606	1.330	2.434	3.104	0.353	0.448	0.731	1.486	0.255
1216	2.55	2.15	23.08	7.653	1.426	2.541	3.670	0.633	0.588	0.941	2.107	0.516
1232	2.44	2.15	28.09	9.165	2.158	3.161	5.117	0.783	0.790	1.292	1.902	0.585
1234	2.19	1.94	34.92		1.341	3.875	3.392	0.327	0.581	0.851	1.652	0.300
1237	2.92	2.04	29.66	8.324	2.536	3.397	5.562	0.580	0.726	1.200	1.411	
1238	2.34	2.04	35.49	8.973	2.257	3.407	5.324	0.533	0.686	1.124	1.278	0.487
1240	2.26	2.10	30.88	9.188	2.552	3.893	5.911	0.880	0.915	1.523	1.743	0.890
1260	2.29	2.10	32.76	10.36	3.480	4.044	7.755	0.917	1.073	1.797	1.429	1.026
1262	2.40	2.10	34.54	11.18	3.648	3.412	7.685	0.894	1.007	1.732	1.298	1.192
1264	2.16	2.10	35.72	11.25	3.980	4.292	8.867	0.950	1.090	1.901	1.035	0.835
1265	2.24	2.05	35.56	10.92	3.710	4.334	8.544	0.977	1.124	1.925	1.161	0.897
1267	2.29	2.10	35.38	11.04	3.900	4.001	8.441	0.936	1.092	1.912	1.191	1.131
1272	2.32	2.00	38.47	9.924	3.716	4.211	8.248	0.674	0.909	1.564	1.056	0.926
1283	2.18	2.00	35.60	10.52	4.545	4.435	10.25	0.913	1.113	2.011	0.932	1.083
1299	2.65	2.14	35.24	12.32	5.453	4.488	12.58	0.758	1.058	1.980	0.716	1.431
1303	3.25	2.13	39.06	11.45	5.187	3.966	13.17	0.694	0.973	1.864	0.616	1.492
1305	2.88	2.14	34.30	8.814	6.002	6.128	13.40	0.728	1.267	2.317	0.660	1.336
1311	2.07	1.85	37.16	11.56	5.850	4.049	13.14	0.876	1.146	2.237	0.485	1.600
1314	3.23	1.98	33.97	13.20	6.162	4.587	15.18	0.795	1.112	2.143	0.503	1.701
1324	3.34	2.04	42.00	11.53	5.776	3.448	14.70	0.615	0.905	1.813	0.357	1.863
1342	2.63	2.08	41.68	8.000	6.913	3.821	18.74	0.408	1.018	1.926	0.257	1.711
1344	1.90	1.90	38.43	12.90	7.370	2.709	20.10	0.543	0.884	1.855	0.173	1.445
1350	2.58	2.16	30.47	10.38	11.16	3.103	27.25	0.466	1.044	1.940	0.177	2.123
1352	1.82	1.80	36.76	11.56	7.478	3.065	20.22	0.594	0.992	2.121	0.136	1.507

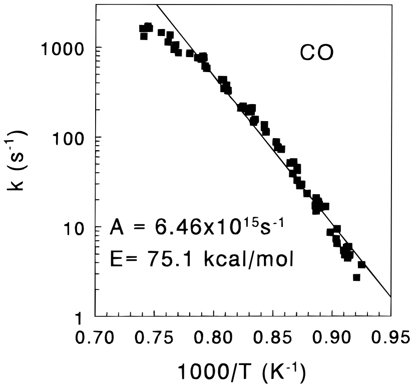

Figure 4. Arrhenius plot of the first-order rate constant of the production of carbon monoxide. The rate constant is calculated from the relation: $k(\text{product}) = k_{\text{total}} \times [\text{product}]_t/([\text{2,5-dimethylfuran}]_0 - [\text{2,5-dimethylfuran}]_t)$.

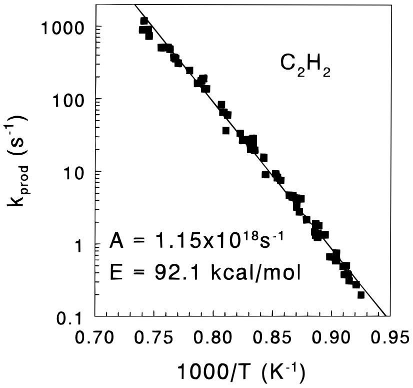

Figure 5. Arrhenius plot of the first-order rate constant of the production of acetylene.

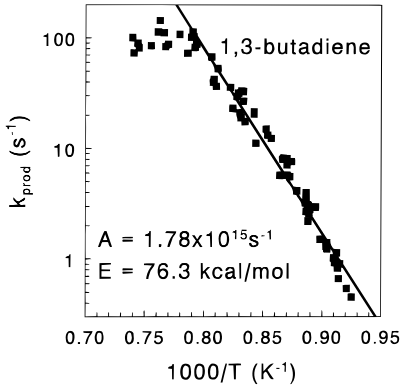

Figure 6. Arrhenius plot of the first-order production of 1,3-butadiene.

C(2) to C(3), with CO elimination and formation of 1-butyne.

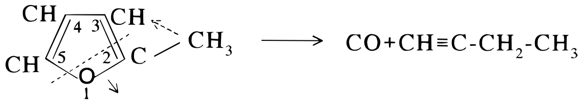

Although interisomerization among the various C_4H_6 isomers does take place,[6] it could be shown, based on computer modeling, that their observed distribution could not be accounted for unless a migration of a methyl group in addition to H-atom migration had to be assumed. Thus the choice of the migration process determined what isomers were formed.

A similar process involving 2,5-dimethylfuran produces C_5H_8 and CO. Since however, there are no H atoms in positions 2 or 5, this process requires a migration of a methyl group from C(2) to C(3) (or from C(5) to C(4)) in the ring.

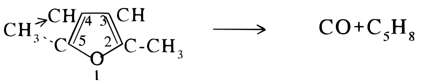

TABLE 2: Arrhenius Parameters for the Production Rates of the Various Products

products	log {A, s^{-1}}	*E*, kcal/mol
total decomposition	16.22	77.5
1,3-butadiene	15.25	76.3
1,2-butadiene	20.37	110.3
1-butyne	15.61	81.6
2-butyne	18.31	103.3
C_4H_4	18.66	94.1
C_4H_2	19.15	106.7
cyclopentadiene	16.55	83.8
1,2,4-pentatriene	15.98	89.0
1,3-pentadiene	14.26	75.4
1,2-pentadiene	14.46	77.4
CO	15.81	75.1
CH_4	13.94	67.4
C_2H_4	18.11	94.7
C_2H_6	18.87	97.1
C_2H_2	18.06	92.1
C_3H_6	16.02	85.2
allene	19.55	104.7
propyne	17.47	91.9
C_6H_6	17.61	82.5
methylfuran	10.80	53.0

As has been shown with 2-methylfuran,[1] this process is considerably slower than the one in which H-atom migrates. Indeed, the concentrations of all the C_5H_8 isomers together are much smaller than those of C_4H_6 in 2-methylfuran. They reach a maximum around 1% of the total distribution whereas the maximum sum of the concentrations of C_4H_6 in the decomposition of 2-methylfuran is around 10%.

To obtain stable C_5H_8 molecules after breaking the 2,5-dimethylfuran ring, additional rearrangements, such as 1,2-, or 1,4-H-atom migrations, must take place in the open C_5H_8 biradical together with CO elimination. These are, for example,

1,2-migration

$$\overset{(1)}{CH_3}-\overset{(2)}{CH^\bullet}-\overset{(3)}{CH}=\overset{(4)}{C^\bullet}-\overset{(5)}{CH_3} \rightarrow$$
$$CH_3-CH=CH-CH=CH_2\ (5\rightarrow 4)\ \text{(1,3-pentadiene)}$$

$$CH_3-CH^\bullet-CH=C^\bullet-CH_3 \rightarrow$$
$$CH_3-CH_2-C\equiv C-CH_3\ \ (3\rightarrow 2)\ \text{(2-pentyne)}$$

$$CH_3-CH^\bullet-CH=C^\bullet-CH_3 \rightarrow$$
$$CH_3-CH=C=CH-CH_3\ (3\rightarrow 4)\ \text{(2,3-pentadiene)}$$

1,4-migration

$$\overset{(1)}{CH_3}-\overset{(2)}{CH^\bullet}-\overset{(3)}{CH}=\overset{(4)}{C^\bullet}-\overset{(5)}{CH_3} \rightarrow$$
$$CH_3-CH_2-CH=C=CH_2\ (5\rightarrow 2)\ \text{(1,2-pentadiene)}$$

GC−MS analysis revealed the presence of four C_5H_8 isomers. Two of them were hidden behind a large peak of cyclopentadiene and could be identified only by the SIM mode of the GC−MS. This can be seen in Figure 7 where the GC peaks corresponding to *m*/*z* 68 (C_5H_8) and 66 (C_5H_6) are shown as a function of retention time. These two isomers were identified as1,3- and 1,2-pentadiene by both retention time and mass

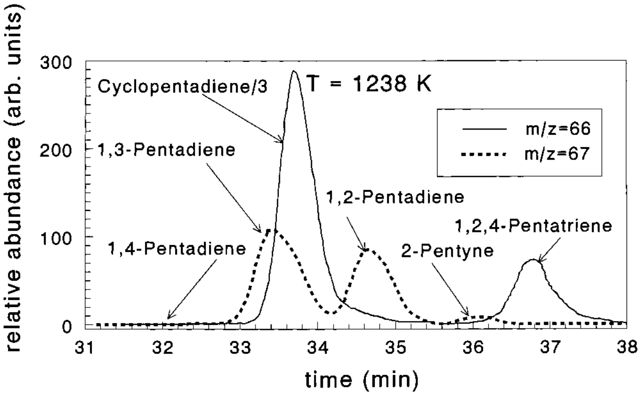

Figure 7. GC-MS chromatogram *m*/*z* 67 (the highest *m*/*z* in C_5H_8 spectrum) and *m*/*z* 66 (C_5H_6) are shown as a function of retention time.

spectrum. Additional two peaks of C_5H_8 that were outside the range of cyclopentadiene appeared in very small quantities. They were identified as 1,4-pentadiene and 2-pentyne. In view of their extremely low concentrations they do not appear neither in the experimental product distribution nor in the computer simulation. Only the two larger C_5H_8 isomers were considered.

An additional unimolecular ring opening channel which yields stable molecules is a simultaneous production of CO, C_2H_4, and C_3H_4.

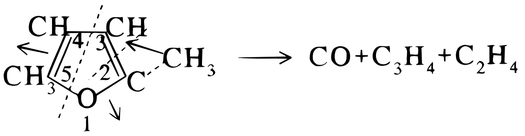

A similar process which produces CO, C_2H_4, and C_2H_2 was assumed to take place in the decomposition of 2-methylfuran.[1] The relatively large concentration of C_2H_2 and C_2H_4 in the decomposition of the latter could not be accounted for unless this process was introduced into the reaction scheme. Indeed, this process involving 2,5-dimethylfuran which yields in addition to CO and C_2H_4 also allene and propyne is practically the only source of the two C_3H_4 isomers. When this channel is removed from the reaction scheme, the concentration of methylacetylene at the low temperature range drops down by about a factor of more than 20. At higher temperatures its concentration drops by only 25% since free radical channels begin to contribute to its production.

It is hard to asses the exact nature of this process. Cleavage of the ring to produce C_3H_4 would leave, following methyl group migration, methylketene. However, we could not identify even traces of the latter among the decomposition product. We believe that methylketene is not really formed in the process. A decomposition to CO and C_2H_4 occurs prior to rearrangement to a stable methylketene molecule. Although the formation of CO and C_2H_4 requires about 10 kcal/mol more than the formation of $CH_3(CH)CO$, entropy considerations enhances the formation of carbon monoxide and ethylene in the process of ring cleavage. It should be mentioned that once methylketene is formed, its further decomposition by H-atom or methyl group elimination is very slow at the temperature range of the present experiment.

2. Unimolecular Processes: Production of Free Radicals. Except for the two unimolecular processes just discussed, all other unimolecular reactions of 2,5-dimethylfuran are associated with production of free radicals. Many of the decomposition products of 2,5-dimethylfuran are formed by free radical reactions. The free radical initiation steps are therefore important steps in the overall decomposition mechanism.

The initiation of free radicals can be divided into two classes of reactions. Those in which the ring is intact and the others where the ring is cleaved to produce unstable intermediates. To the first class belongs the ejection of a H atom from the methyl group in the molecule

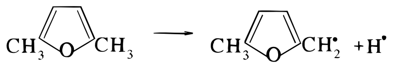

and ejection of a methyl group from the ring

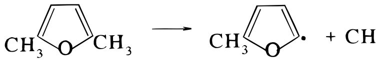

The C−H bond in the methyl group is the weakest bond in the molecule. It is a sp^3 bond which is weakened by the $\beta-\gamma$ C═C double bond in the ring. It is estimated as $D(CH_2-H)$ ∼88 kcal/mol, similar to the equivalent process in toluene.[7] The ejection of a hydrogen atom from the methyl group has a reaction coordinate degeneracy of 6 so it is an important initiation reaction that affects almost all the reaction products in the system. The ejection of a methyl group from the ring, on the other hand, is slower. The $C-CH_3$ bond is strengthen by the $\alpha-\beta$ double bond in the ring in comparison to a normal $C-CH_3$ bond and it is estimated as $D(C-CH_3)$ ∼98 kcal/mol. Its contribution to the overall production of free radicals is much smaller than that of the H-atom ejection reaction. Ejection of a hydrogen atom from the ring is very slow in view of the high C−H bond energy, $D(C-H)$ ∼112 kcal/mol.

In the second class of reactions the ring opens in different locations. These reactions are shown in the kinetic scheme (Table 3), as reactions 7−9.

Reactions similar to reactions 7 and 8 involving 2,5-dimethylfuran appear in the decomposition scheme of 2-methylfuran.[1] We have added here an additional decomposition reaction:

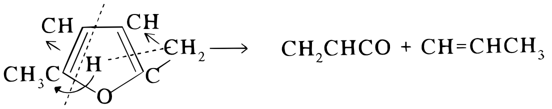

This reaction involves a 1,2-methyl group migration together with a 1,4-H-atom migration from the migrating methyl to a carbon atom in the ring. Since CH_2CHCO further decomposes to C_2H_3 and CO quite rapidly, the production of acetylene, which is formed by the dissociation of C_2H_3, highly depends on this reaction. In fact, without its presence in the scheme, the concentration of acetylene, which is among the species with the highest concentrations, cannot be accounted for.

3. Consecutive Free Radical Reactions. Almost all the reactions that take part in the kinetic scheme of 2,5-dimethylfuran decomposition are reactions that involve free radicals. In addition to the unimolecular decompositions of the reactant that produce free radicals, there are consecutive steps such as abstractions, recombinations, dissociative attachments and unimolecular decompositions of unstable, free radical, intermediates.

a. Abstractions. We have introduced into the reaction scheme abstraction reactions involving H atoms and free radicals containing up to three carbon atoms namely, $CH_3^{\bullet}$, $C_3H_3^{\bullet}$, and $C_3H_5^{\bullet}$. Abstractions from 2,5-dimethylfuran by relatively high concentration free radicals such as $C_4H_5^{\bullet}$ and $C_5H_5^{\bullet}$ were also

TABLE 3: Reactions Scheme for Decomposition of 2,5-Dimethylfuran[a]

reaction number	reaction	*A*	*E*	k_f	k_r	ΔS^0	ΔH^0	ref
1	DMF → CO + 1,3-pentadiene	1.0×10^{15}	80.0	10	0.16	43.9	15.9	this work
2	DMF → CO + 1,2-pentadiene	1.6×10^{15}	80.0	17	22	47.9	31.9	this work
3	DMF → p-$C_3H_4 + C_2H_4$ + CO	1.5×10^{15}	79.5	19	4.1×10^{3}	76.8	52.0	est[b]
4	DMF → a-$C_3H_4 + C_2H_4$ + CO	8.0×10^{14}	82.5	3.0	2.0×10^{3}	75.8	53.5	est
5	DMF → DMF(R)$^\bullet$ + H$^\bullet$	1.6×10^{16}	86.0	14.8	4.8×10^{14}	31.8	88.4	est
6	DMF → MF(R2)$^\bullet$ + $CH_3^\bullet$	3.0×10^{16}	96.0	0.49	6.8×10^{13}	36.9	98.4	est
7	DMF → $CH_3CO^\bullet + CH_2^\bullet{-}C{\equiv}C{-}CH_3$	2.0×10^{16}	85.0	28	5.5×10^{9}	52.9	84.9	est
8	DMF → $CH_3CO^\bullet + (CHCCHCH_3)^\bullet$	2.0×10^{16}	85.0	28	1.6×10^{10}	50.7	84.8	est
9	DMF → $C_3H_3O^\bullet + C_3H_5^\bullet$	8.0×10^{15}	82.0	37	4.8×10^{7}	59.4	80.5	est
10	DMF + H$^\bullet$ → 1,3-butadiene + $CH_3CO^\bullet$	3.0×10^{14}	6.0	2.7×10^{13}	2.4×10^{7}	18.8	−11.2	est
11	DMF + H$^\bullet$ → 2-butyne + $CH_3CO^\bullet$	3.0×10^{13}	15.0	7.2×10^{10}	4.0×10^{6}	16.8	−3.3	est
12	DMF + H$^\bullet$ → 1,2-butadiene + $CH_3CO^\bullet$	7.5×10^{13}	11.0	9.0×10^{11}	6.1×10^{7}	20.3	1.6	est
13	DMF + H$^\bullet$ → 1-butyne + $CH_3CO^\bullet$	1.0×10^{14}	10.0	1.8×10^{12}	2.0×10^{8}	20.0	2.3	est
14	DMF + H$^\bullet$ → $CH_3^\bullet$ + MF	3.0×10^{14}	6.0	2.7×10^{13}	5.9×10^{9}	5.8	−13.7	est
15	DMF + H$^\bullet$ → $C_3H_5^\bullet + C_2H_4$ + CO	2.0×10^{14}	8.0	8.0×10^{12}	3.1×10^{5}	52.1	−5.9	est
16	DMF + H$^\bullet$ → DMF(R)$^\bullet$ + H_2	1.0×10^{14}	8.0	4.0×10^{12}	2.9×10^{8}	4.2	−18.5	est
17	DMF + $CH_3^\bullet$ → DMF(R)$^\bullet$ + CH_4	3.0×10^{13}	15.0	7.2×10^{10}	9.9×10^{7}	−2.4	−19.3	est
18	DMF + $C_3H_3^\bullet$ → DMF(R)$^\bullet$ + p-C_3H_4	8.0×10^{11}	10.0	1.4×10^{10}	3.9×10^{9}	−1.1	−4.7	est
19	DMF + $C_3H_3^\bullet$→ DMF(R)$^\bullet$ + a-C_3H_4	8.0×10^{11}	10.0	1.4×10^{10}	1.2×10^{10}	−2.2	−3.2	est
20	DMF + $C_3H_5^\bullet$ → DMF(R)$^\bullet$ + C_3H_6	8.0×10^{11}	14.0	2.9×10^{9}	3.8×10^{9}	−2.1	−2.0	est
21	DMF + $CH_2^\bullet{-}C{\equiv}C{-}CH_3$ →DMF(R)$^\bullet$ + 2-butyne	8.0×10^{11}	15.0	1.9×10^{9}	1.8×10^{10}	−4.3	0.2	est
22	DMF + $(CHCCHCH_3)^\bullet$ →DMF(R)$^\bullet$ + 1-butyne	5.0×10^{12}	10.0	8.9×10^{10}	5.6×10^{11}	1.1	6.0	est
23	DMF + $(c{-}C_5H_5)^\bullet$ → DMF(R)$^\bullet$ + cyclopentadiene	5.0×10^{11}	15.0	1.2×10^{9}	4.4×10^{9}	−0.5	2.6	est
24	MF → 2-butyne + CO	2.3×10^{15}	85.1	3.0	4.2	42.0	24.7	1
25	MF → 1,3-butadiene + CO	3.5×10^{15}	79.5	44	0.97	43.9	16.8	1
26	MF → 1,2-butadiene + CO	4.5×10^{15}	85.1	6.0	10	45.5	29.6	1
27	MF → 1-butyne + CO	2.8×10^{15}	79.5	35	99	45.2	30.3	1
28	MF → p-$C_3H_4 + CH_2CO$	5.8×10^{15}	82.9	19	6.6×10^{4}	46.3	49.5	1
29	MF → $C_2H_2 + C_2H_4$ + CO	1.8×10^{15}	79.5	22	4.0×10^{4}	76.7	57.2	1
30	MF → $CH_3CO^\bullet + C_3H_3^\bullet$	4.0×10^{16}	90.5	6.0	6.1×10^{10}	52.7	94.5	1
31	MF → $HCO^\bullet + CH^\bullet{=}CH{-}CH{=}CH_2$	4.0×10^{16}	106.0	1.2×10^{-2}	6.1×10^{10}	51.4	108.4	1
32	MF → MF(R1)$^\bullet$ + H$^\bullet$	8.0×10^{15}	86.0	7.4	1.2×10^{14}	34.8	90.5	1
33	MF + H$^\bullet$ → MF(R1)$^\bullet$ + H_2	3.0×10^{14}	9.0	8.0×10^{12}	3.0×10^{8}	7.2	−16.4	1
34	MF + $CH_3^\bullet$ → MF(R1)$^\bullet$ + CH_4	1.0×10^{13}	13.0	5.3×10^{10}	3.8×10^{7}	0.6	−17.3	1
35	MF + $C_3H_3^\bullet$ → MF(R1)$^\bullet$ + p-C_3H_4	5.0×10^{12}	10.0	8.9×10^{10}	1.2×10^{10}	1.9	−2.6	1
36	MF + $C_3H_3^\bullet$ → MF(R1)$^\bullet$ + a-C_3H_4	5.0×10^{12}	10.0	8.9×10^{10}	3.8×10^{10}	0.8	−1.1	1
37	MF + $C_3H_5^\bullet$ → MF(R1)$^\bullet$ + C_3H_6	8.0×10^{11}	14.0	2.9×10^{9}	2.0×10^{9}	0.9	0.1	1
38	MF + H$^\bullet$ → furan + $CH_3^\bullet$	3.0×10^{14}	6.0	2.7×10^{13}	1.1×10^{10}	7.5	−10.0	1
39	MF → furan(R)$^\bullet$ + $CH_3^\bullet$	1.5×10^{16}	90.0	2.8	1.8×10^{13}	34.5	87.8	est
40	DMF(R)$^\bullet$ → $CH_2{=}CH{-}CH{=}CH{-}CH_2^\bullet$ + CO	1.0×10^{15}	48.0	4.1×10^{6}	4.2×10^{5}	41.7	17.9	est
41	DMF(R)$^\bullet$ → $CH_3CO^\bullet + C_4H_4$	5.0×10^{15}	56.0	8.1×10^{5}	1.8×10^{10}	48.4	56.8	est
42	DMF(R)$^\bullet$ → p-$C_3H_4 + C_2H_3^\bullet$ + CO	3.3×10^{15}	77.0	1.1×10^{2}	1.3×10^{8}	80.3	77.7	est
43	MF(R1)$^\bullet$ → CO + $(CH_2{=}CCHCH_2)^\bullet$	4.0×10^{15}	64.0	2.6×10^{4}	1.3×10^{5}	40.6	26.0	1
44	MF(R1)$^\bullet$ → CO + $CH^\bullet{=}CH{-}CH{=}CH_2$	2.3×10^{15}	71.0	8.7×10^{2}	1.0×10^{5}	41.8	35.5	1
45	MF(R1)$^\bullet$ → $CH_2CO + C_3H_3^\bullet$	2.3×10^{15}	64.0	1.5×10^{4}	3.8×10^{8}	44.4	52.1	1
46	MF(R1)$^\bullet$ → $HCO^\bullet + C_4H_4$	2.3×10^{15}	64.0	1.5×10^{4}	4.2×10^{10}	45.4	65.1	1
47	MF(R1)$^\bullet$ → $C_2H_2 + C_2H_3^\bullet$ + CO	3.3×10^{15}	76.7	1.3×10^{2}	2.6×10^{9}	77.1	80.9	1
48	MF(R2)$^\bullet$ + H$^\bullet$ → MF	2.0×10^{14}	0.0	2.0×10^{14}	3.2×10^{-4}	−31.2	−112.1	est
49	MF(R2)$^\bullet$ → CO + $CH_2^\bullet{-}C{\equiv}C{-}CH_3$	2.0×10^{15}	70.0	1.2×10^{3}	9.1×10^{-3}	46.9	0.8	est
50	furan(R)$^\bullet$ + H$^\bullet$ → furan	2.0×10^{14}	0.0	2.0×10^{14}	1.3×10^{-2}	−27.0	−97.8	est
51	furan(R)$^\bullet$ → CO + $C_3H_3^\bullet$	1.7×10^{15}	65.0	7.4×10^{3}	64	49.2	21.0	est
52	2-butyne → 1,3-butadiene	3.0×10^{13}	65.0	1.3×10^{2}	2.0	1.9	−7.9	6
53	1,2-butadiene → 1,3-butadiene	3.0×10^{13}	65.0	1.3×10^{2}	1.7	−1.6	−12.8	6
54	1,2-butadiene → 2-butyne	3.0×10^{13}	65.0	1.3×10^{2}	1.1×10^{2}	−3.5	−4.9	6
55	1-butyne → 1,2-butadiene	2.0×10^{13}	65.0	87	53	0.4	−0.8	6
56	$CH_2^\bullet{-}C{\equiv}C{-}CH_3$ + H$^\bullet$ → 2-butyne	5.0×10^{13}	0.0	5.0×10^{13}	14.1	−36.1	−88.2	1*[c]
57	$CH_2^\bullet{-}C{\equiv}C{-}CH_3$ + H$^\bullet$ → 1,2-butadiene	5.0×10^{13}	0.0	5.0×10^{13}	17.1	−32.6	−83.3	1*
58	$(CHCCHCH_3)^\bullet$ + H$^\bullet$ → 1,2-butadiene	5.0×10^{13}	0.0	5.0×10^{13}	6.0	−30.4	−83.2	1*
59	$(CHCCHCH_3)^\bullet$ + H$^\bullet$ → 1-butyne	5.0×10^{13}	0.0	5.0×10^{13}	9.7	−30.7	−82.5	1*
60	$CH{\equiv}C{-}CH_2{-}CH_2^\bullet$ + H$^\bullet$ → 1-butyne	5.0×10^{13}	0.0	5.0×10^{13}	1.7	−33.1	−89.8	1*
61	$CH^\bullet{=}CH{-}CH{=}CH_2$ + H$^\bullet$ → 1,3-butadiene	5.0×10^{13}	0.0	5.0×10^{13}	5.5×10^{-4}	−32.7	−109.2	1*
62	$(CH_2{=}CCHCH_2)^\bullet$ + H$^\bullet$ → 1,2-butadiene	5.0×10^{13}	0.0	5.0×10^{13}	1.1	−29.9	−86.9	1*
63	$(CH_2{=}CCHCH_2)^\bullet$ + H$^\bullet$ → 1,3-butadiene	5.0×10^{13}	0.0	5.0×10^{13}	1.3×10^{-2}	−31.4	−99.7	1*
64	$(CHCCHCH_3)^\bullet$ → H$^\bullet$ + C_4H_4	1.0×10^{14}	58.0	7.2×10^{3}	9.3×10^{12}	29.6	60.4	1*
65	$CH_2^\bullet{-}C{\equiv}C{-}CH_3$ → H$^\bullet$ + C_4H_4	2.0×10^{14}	54.0	7.3×10^{4}	2.7×10^{14}	27.4	60.3	1*
66	$CH{\equiv}C{-}CH_2{-}CH_2^\bullet$ → H$^\bullet$ + C_4H_4	1.0×10^{14}	50.0	1.8×10^{5}	4.0×10^{13}	27.2	53.1	1*
67	$CH^\bullet{=}CH{-}CH{=}CH_2$ → H$^\bullet$ + C_4H_4	1.0×10^{14}	45.0	1.4×10^{6}	1.3×10^{13}	28.8	47.2	1
68	$(CH_2{=}CCHCH_2)^\bullet$ → H$^\bullet$ + C_4H_4	1.0×10^{14}	53.0	5.4×10^{4}	1.2×10^{13}	30.1	56.7	1
69	2-butyne + H$^\bullet$ → $CH_2^\bullet{-}C{\equiv}C{-}CH_3 + H_2$	6.0×10^{14}	6.8	3.9×10^{13}	3.0×10^{8}	8.4	−18.7	1
70	1,3-butadiene + H$^\bullet$ → $CH^\bullet{=}CH{-}CH{=}CH_2 + H_2$	4.0×10^{14}	6.8	2.6×10^{13}	5.2×10^{12}	5.1	2.4	1
71	1,3-butadiene + H$^\bullet$ → $(CH_2{=}CCHCH_2)^\bullet + H_2$	2.0×10^{14}	6.8	1.3×10^{13}	1.1×10^{11}	3.8	−7.2	1
72	1,2-butadiene + H$^\bullet$ → $CH_2^\bullet{-}C{\equiv}C{-}CH_3 + H_2$	1.0×10^{14}	6.8	6.5×10^{12}	4.1×10^{7}	4.9	−23.5	1

TABLE 3: Continued

reaction number	reaction	A	E	k_f	k_r	ΔS^0	ΔH^0	ref
73	1,2-butadiene $+ H^\bullet \rightarrow (CH_2{=}CCHCH_2)^\bullet + H_2$	3.0×10^{14}	6.8	1.9×10^{13}	2.1×10^{9}	2.2	−19.9	1
74	1-butyne $+ H^\bullet \rightarrow (CHCCHCH_3)^\bullet + H_2$	2.0×10^{14}	6.8	1.3×10^{13}	1.5×10^{8}	3.1	−24.4	1
75	1-butyne $+ H^\bullet \rightarrow CH{\equiv}C{-}CH_2{-}CH_2^\bullet + H_2$	3.0×10^{14}	6.8	1.9×10^{13}	1.3×10^{9}	5.5	−17.1	1
76	2-butyne $+ CH_3^\bullet \rightarrow CH_4 + CH_2^\bullet{-}C{\equiv}C{-}CH_3$	6.0×10^{13}	11.5	5.9×10^{11}	8.8×10^{7}	1.9	−19.5	1
77	1,3-butadiene $+ CH_3^\bullet \rightarrow CH_4 + (CH_2{=}CCHCH_2)^\bullet$	4.0×10^{13}	11.5	3.9×10^{11}	6.2×10^{10}	−2.8	−8.0	1
78	1,3-butadiene $+ CH_3^\bullet \rightarrow CH_4 + CH^\bullet{=}CH{-}CH{=}CH_2$	2.0×10^{13}	11.5	2.0×10^{11}	7.5×10^{11}	−1.5	1.5	1
79	1,2-butadiene $+ CH_3^\bullet \rightarrow CH_4 + CH_2^\bullet{-}C{\equiv}C{-}CH_3$	1.0×10^{13}	11.5	9.8×10^{10}	1.2×10^{7}	−1.6	−24.4	1
80	1,2-butadiene $+ CH_3^\bullet \rightarrow CH_4 + (CH_2{=}CCHCH_2)^\bullet$	3.0×10^{13}	11.5	2.9×10^{11}	5.9×10^{8}	−4.3	−20.8	1
81	1-butyne $+ CH_3^\bullet \rightarrow CH_4 + (CHCCHCH_3)^\bullet$	2.0×10^{13}	11.5	2.0×10^{11}	4.3×10^{7}	−3.5	−25.3	1
82	1-butyne $+ CH_3^\bullet \rightarrow CH_4 + CH{\equiv}C{-}CH_2{-}CH_2^\bullet$	3.0×10^{13}	11.5	2.9×10^{11}	3.7×10^{8}	−1.1	−18.0	1
83	2-butyne $+ C_3H_3^\bullet \rightarrow p\text{-}C_3H_4 + CH_2^\bullet{-}C{\equiv}C{-}CH_3$	5.0×10^{12}	11.5	4.9×10^{10}	1.4×10^{9}	3.1	−4.9	1*
84	1,3-butadiene $+ C_3H_3^\bullet \rightarrow p\text{-}C_3H_4 + (CH_2{=}CCHCH_2)^\bullet$	5.0×10^{12}	12.0	4.0×10^{10}	1.2×10^{12}	−1.5	6.6	1*
85	1,3-butadiene $+ C_3H_3^\bullet \rightarrow p\text{-}C_3H_4 + CH^\bullet{=}CH{-}CH{=}CH_2$	5.0×10^{12}	17.0	5.3×10^{9}	4.1×10^{12}	−0.3	16.1	1*
86	1,2-butadiene $+ C_3H_3^\bullet \rightarrow p\text{-}C_3H_4 + CH_2^\bullet{-}C{\equiv}C{-}CH_3$	5.0×10^{12}	12.0	4.0×10^{10}	9.6×10^{8}	−0.4	−9.8	1
87	1,2-butadiene $+ C_3H_3^\bullet \rightarrow p\text{-}C_3H_4 + (CH_2{=}CCHCH_2)^\bullet$	5.0×10^{12}	12.0	4.0×10^{10}	1.6×10^{10}	−3.1	−6.2	1*
88	1-butyne $+ C_3H_3^\bullet \rightarrow p\text{-}C_3H_4 + (CHCCHCH_3)^\bullet$	5.0×10^{12}	12.0	4.0×10^{10}	1.7×10^{9}	−2.2	−10.6	1*
89	1-butyne $+ C_3H_3^\bullet \rightarrow p\text{-}C_3H_4 + CH{\equiv}C{-}CH_2{-}CH_2^\bullet$	5.0×10^{12}	12.0	4.0×10^{10}	1.0×10^{10}	0.1	−3.3	1*
90	2-butyne $+ C_3H_3^\bullet \rightarrow a\text{-}C_3H_4 + CH_2^\bullet{-}C{\equiv}C{-}CH_3$	2.0×10^{12}	11.5	2.0×10^{10}	1.7×10^{9}	2.1	−3.4	1,est
91	1,3-butadiene $+ C_3H_3^\bullet \rightarrow a\text{-}C_3H_4 + (CH_2{=}CCHCH_2)^\bullet$	2.0×10^{12}	12.0	1.6×10^{10}	1.5×10^{12}	−2.6	8.1	1,est
92	1,3-butadiene $+ C_3H_3^\bullet \rightarrow a\text{-}C_3H_4 + CH^\bullet{=}CH{-}CH{=}CH_2$	2.0×10^{12}	18.0	1.4×10^{9}	3.3×10^{12}	−1.3	17.6	1,est
93	1,2-butadiene $+ C_3H_3^\bullet \rightarrow a\text{-}C_3H_4 + CH_2^\bullet{-}C{\equiv}C{-}CH_3$	2.0×10^{12}	12.0	1.6×10^{10}	1.2×10^{9}	−1.4	−8.3	1,est
94	1,2-butadiene $+ C_3H_3^\bullet \rightarrow a\text{-}C_3H_4 + (CH_2{=}CCHCH_2)^\bullet$	2.0×10^{12}	12.0	1.6×10^{10}	1.9×10^{10}	−4.1	−4.7	1,est
95	1-butyne $+ C_3H_3^\bullet \rightarrow a\text{-}C_3H_4 + (CHCCHCH_3)^\bullet$	2.0×10^{12}	12.0	1.6×10^{10}	2.1×10^{9}	−3.3	−9.2	1,est
96	1-butyne $+ C_3H_3^\bullet \rightarrow a\text{-}C_3H_4 + CH{\equiv}C{-}CH_2{-}CH_2^\bullet$	2.0×10^{12}	12.0	1.6×10^{10}	1.2×10^{10}	−0.9	−1.8	1,est
97	2-butyne $+ C_3H_5^\bullet \rightarrow C_3H_6 + CH_2^\bullet{-}C{\equiv}C{-}CH_3$	8.0×10^{11}	12.0	6.4×10^{9}	9.3×10^{8}	2.1	−2.2	est
98	1,3-butadiene $+ C_3H_5^\bullet \rightarrow C_3H_6 + (CH_2{=}CCHCH_2)^\bullet$	8.0×10^{11}	15.0	1.9×10^{9}	2.9×10^{11}	−2.5	9.3	est
99	1,3-butadiene $+ C_3H_5^\bullet \rightarrow C_3H_6 + CH^\bullet{=}CH{-}CH{=}CH_2$	8.0×10^{11}	25.0	3.4×10^{7}	1.3×10^{11}	−1.3	18.8	est
100	1,2-butadiene $+ C_3H_5^\bullet \rightarrow C_3H_6 + CH_2^\bullet{-}C{\equiv}C{-}CH_3$	8.0×10^{11}	12.0	6.4×10^{9}	7.5×10^{8}	−1.4	−7.1	est
101	1,2-butadiene $+ C_3H_5^\bullet \rightarrow C_3H_6 + (CH_2{=}CCHCH_2)^\bullet$	8.0×10^{11}	12.0	6.4×10^{9}	1.3×10^{10}	−4.1	−3.5	est
102	1-butyne $+ C_3H_5^\bullet \rightarrow C_3H_6 + (CHCCHCH_3)^\bullet$	8.0×10^{11}	12.0	6.4×10^{9}	1.3×10^{9}	−3.2	−7.9	est
103	1-butyne $+ C_3H_5^\bullet \rightarrow C_3H_6 + CH{\equiv}C{-}CH_2{-}CH_2^\bullet$	8.0×10^{11}	12.0	6.4×10^{9}	7.8×10^{9}	−0.9	−0.6	est
104	1,3-butadiene $\rightarrow C_4H_4 + H_2$	2.0×10^{13}	75.0	1.6	2.9×10^{6}	33.9	49.6	6
105	1,3-butadiene $\rightarrow C_2H_2 + C_2H_4$	1.2×10^{13}	66.0	35	3.0×10^{6}	32.7	40.4	6
106	1,3-butadiene $+ H^\bullet \rightarrow C_2H_3^\bullet + C_2H_4$	2.0×10^{14}	5.0	2.7×10^{13}	1.0×10^{12}	8.9	3.0	est
107	2-butyne $\rightarrow C_3H_3^\bullet + CH_3^\bullet$	1.0×10^{16}	82.0	46	1.9×10^{12}	41.7	84.1	est
108	1,2-butadiene $\rightarrow C_3H_3^\bullet + CH_3^\bullet$	1.0×10^{16}	79.0	1.5×10^{2}	5.0×10^{12}	38.2	79.2	1
109	1-butyne $\rightarrow C_3H_3^\bullet + CH_3^\bullet$	1.0×10^{16}	78.0	2.3×10^{2}	4.6×10^{12}	38.5	78.4	1
110	1,3-pentadiene $\rightarrow c\text{-}C_5H_6 + H_2$	1.0×10^{13}	64.5	53	1.9×10^{7}	32.1	43.3	17
111	1,3-pentadiene $\rightarrow CH_2{=}CH{-}CH{=}CH{-}CH_2^\bullet + H^\bullet$	3.2×10^{15}	90.0	0.59	1.3×10^{14}	29.7	90.4	est
112	1,3-pentadiene $\rightarrow CH^\bullet{=}CH{-}CH{=}CH_2 + CH_3^\bullet$	1.0×10^{16}	97.0	0.11	3.1×10^{12}	38.5	96.4	est
113	1,3-pentadiene $+ H^\bullet \rightarrow CH_2{=}CH{-}CH{=}CH{-}CH_2^\bullet + H_2$	2.0×10^{14}	7.0	1.2×10^{13}	5.6×10^{9}	2.0	−16.5	est
114	1,3-pentadiene $+ CH_3^\bullet \rightarrow CH_2{=}CH{-}CH{=}CH{-}CH_2^\bullet + CH_4$	2.0×10^{13}	11.5	2.0×10^{11}	1.8×10^{9}	−4.5	−17.4	est
115	1,3-pentadiene $+ C_3H_3^\bullet \rightarrow CH_2{=}CH{-}CH{=}CH{-}CH_2^\bullet + a\text{-}C_3H_4$	5.0×10^{12}	12.0	4.0×10^{10}	2.1×10^{11}	−4.3	−1.2	est
116	1,3-pentadiene $+ C_3H_3^\bullet \rightarrow CH_2{=}CH{-}CH{=}CH{-}CH_2^\bullet + p\text{-}C_3H_4$	5.0×10^{12}	12.0	4.0×10^{10}	7.1×10^{10}	−3.3	−2.7	est
117	1,3-pentadiene $+ C_3H_5^\bullet \rightarrow CH_2{=}CH{-}CH{=}CH{-}CH_2^\bullet + C_3H_6$	8.0×10^{11}	12.0	6.4×10^{9}	5.6×10^{10}	−4.3	0.0	est
118	1,2-pentadiene $\rightarrow (CH_2{=}CCHCH_2)^\bullet + CH_3^\bullet$	1.0×10^{16}	71.0	3.9×10^{3}	5.3×10^{13}	33.2	70.9	est
119	1,2-pentadiene $\rightarrow C_3H_3^\bullet + C_2H_5^\bullet$	1.0×10^{16}	75.0	7.7×10^{2}	8.2×10^{12}	37.0	74.9	est
120	1,2-pentadiene $+ H^\bullet \rightarrow CH_2{=}C{=}CH{-}CH^\bullet{-}CH_3 + H_2$	2.0×10^{14}	7.0	1.2×10^{13}	1.6×10^{9}	−0.3	−22.5	est
121	1,2-pentadiene $+ CH_3^\bullet \rightarrow CH_2{=}C{=}CH{-}CH^\bullet{-}CH_3 + CH_4$	2.0×10^{13}	11.5	2.0×10^{11}	5.1×10^{8}	−6.9	−23.4	est
122	1,2-pentadiene $+ C_3H_3^\bullet \rightarrow CH_2{=}C{=}CH{-}CH^\bullet{-}CH_3 + a\text{-}C_3H_4$	5.0×10^{12}	12.0	4.0×10^{10}	6.3×10^{10}	−6.7	−7.2	est
123	1,2-pentadiene $+ C_3H_3^\bullet \rightarrow CH_2{=}C{=}CH{-}CH^\bullet{-}CH_3 + p\text{-}C_3H_4$	5.0×10^{12}	12.0	4.0×10^{10}	2.1×10^{10}	−5.6	−8.7	est
124	1,2-pentadiene $+ C_3H_5^\bullet \rightarrow CH_2{=}C{=}CH{-}CH^\bullet{-}CH_3 + C_3H_6$	8.0×10^{11}	12.0	6.4×10^{9}	1.6×10^{10}	−6.6	−6.0	est
125	$CH_2{=}C{=}CH{-}CH^\bullet\text{-}CH_3 \rightarrow CH_2{=}C{=}CH{-}CH{=}CH_2 + H^\bullet$	1.0×10^{14}	50.0	1.8×10^{5}	5.8×10^{12}	28.4	49.8	est
126	$CH_2{=}CH{-}CH{=}CH{-}CH_2^\bullet \rightarrow$ cyclopentadiene $+ H^\bullet$	1.0×10^{13}	40.0	1.0×10^{6}	1.8×10^{12}	18.6	30.4	est
127	cyclopentadiene $\rightarrow (c\text{-}C_5H_5)^\bullet + H^\bullet$	1.1×10^{15}	85.0	1.5	1.3×10^{13}	32.3	85.8	18
128	cyclopentadiene $+ H^\bullet \rightarrow (c\text{-}C_5H_5)^\bullet + H_2$	9.3×10^{13}	5.4	1.1×10^{13}	2.1×10^{8}	4.7	−21.1	19,20
129	cyclopentadiene $+ H^\bullet \rightarrow C_2H_3^\bullet + a\text{-}C_3H_4$	3.0×10^{14}	31.0	1.1×10^{9}	2.2×10^{10}	18.9	30.9	est
130	cyclopentadiene $+ H^\bullet \rightarrow C_2H_3^\bullet + p\text{-}C_3H_4$	3.0×10^{14}	30.0	1.7×10^{9}	1.1×10^{10}	19.9	29.5	est
131	cyclopentadiene $+ CH_3^\bullet \rightarrow CH_4 + (c\text{-}C_5H_5)^\bullet$	2.0×10^{13}	12.0	1.6×10^{11}	5.9×10^{7}	−1.9	−22.0	est
132	cyclopentadiene $+ C_3H_3^\bullet \rightarrow a\text{-}C_3H_4 + (c\text{-}C_5H_5)^\bullet$	2.0×10^{12}	14.0	7.1×10^{9}	1.6×10^{9}	−1.7	−5.8	est
133	cyclopentadiene $+ C_3H_3^\bullet \rightarrow p\text{-}C_3H_4 + (c\text{-}C_5H_5)^\bullet$	2.0×10^{12}	12.0	1.6×10^{10}	1.2×10^{9}	−0.6	−7.3	est
134	cyclopentadiene $+ C_3H_5^\bullet \rightarrow (c\text{-}C_5H_5)^\bullet + C_3H_6$	8.0×10^{11}	12.0	6.4×10^{9}	2.3×10^{9}	−1.6	−4.6	est
135	$CH_2{=}C{=}CH{-}CH{=}CH_2 \rightarrow C_3H_3^\bullet + C_2H_3^\bullet$	1.0×10^{16}	92.0	0.82	1.4×10^{12}	41.4	93.1	est
136	$CH_2{=}C{=}CH{-}CH{=}CH_2 + H^\bullet \rightarrow C_3H_3^\bullet + C_2H_4$	1.0×10^{14}	5.4	1.1×10^{13}	1.1×10^{8}	6.1	−21.0	est
137	$CH_2{=}C{=}CH{-}CH{=}CH_2 + CH_3^\bullet \rightarrow C_3H_3^\bullet + C_3H_6$	2.0×10^{13}	12.0	1.6×10^{11}	2.3×10^{9}	1.0	−9.2	est
138	$(c\text{-}C_5H_5)^\bullet \rightarrow CH_2^\bullet\text{-}CH{=}CH{-}CH{\equiv}CH$	5.0×10^{13}	33.3	7.5×10^{7}	4.8×10^{11}	9.0	33.0	9
139	$CH_2^\bullet{-}CH{=}CH{-}CH{\equiv}CH \rightarrow C_3H_3^\bullet + C_2H_2$	$1.3 \times 10^{23}T^{-3.11}$	44.4	5.3×10^{5}	1.6×10^{10}	35.4	41.2	9
140	$a\text{-}C_3H_4 \rightarrow p\text{-}C_3H_4$	1.5×10^{13}	60.4	4.1×10^{2}	1.3×10^{2}	1.0	−1.5	21
141	$a\text{-}C_3H_4 + Ar \rightarrow C_3H_3^\bullet + H^\bullet + Ar$	4.1×10^{17}	75.0	3.1×10^{4}	1.2×10^{18}	34.0	91.6	12
142	$p\text{-}C_3H_4 + Ar \rightarrow C_3H_3^\bullet + H^\bullet + Ar$	4.7×10^{17}	80.0	4.9×10^{3}	5.8×10^{17}	33.0	93.1	22
143	$p\text{-}C_3H_4 + H^\bullet \rightarrow C_3H_5^\bullet$	2.0×10^{13}	2.4	7.6×10^{12}	1.4×10^{3}	−24.7	−57.9	11
144	$a\text{-}C_3H_4 + H^\bullet \rightarrow C_3H_5^\bullet$	2.0×10^{13}	2.4	7.6×10^{12}	4.6×10^{2}	−23.7	−59.4	11

TABLE 3: Continued

reaction number	reaction	A	E	k_f	k_r	ΔS^0	ΔH^0	ref
145	$p\text{-}C_3H_4 + C_3H_3 \rightarrow C_6H_6 + H^{\bullet}$	1.5×10^{13}	6.0	1.3×10^{12}	4.7×10^{8}	−27.2	−53.7	est
146	$C_2H_2 + C_2H_2 \rightarrow C_4H_4$	6.2×10^{13}	41.1	4.1×10^{6}	1.0×10^{2}	−30.3	−35.5	12
147	$C_2H_2 + C_2H_2 \rightarrow C_4H_3^{\bullet} + H^{\bullet}$	1.0×10^{12}	66.0	2.9	2.8×10^{12}	2.7	71.9	23
148	$C_2H_2 + CH_3^{\bullet} \rightarrow C_3H_5^{\bullet}$	6.0×10^{11}	7.7	2.7×10^{10}	2.5×10^{3}	−30.3	−49.4	24
149	$C_2H_2 + CH_3^{\bullet} \rightarrow p\text{-}C_3H_4 + H^{\bullet}$	$2.7 \times 10^{18}T^{-1.96}$	20.6	5.8×10^{8}	3.0×10^{11}	−5.6	8.5	28
150	$C_2H_2 + CH_3^{\bullet} \rightarrow a\text{-}C_3H_4 + H^{\bullet}$	$6.7 \times 10^{19}T^{-2.08}$	31.6	7.3×10^{7}	1.2×10^{11}	−6.6	10.0	28
151	$C_2H_3^{\bullet} + Ar \rightarrow C_2H_2 + H^{\bullet} + Ar$	3.0×10^{15}	32.0	7.6×10^{9}	1.7×10^{16}	23.8	37.4	12
152	$C_2H_3^{\bullet} + H^{\bullet} \rightarrow C_2H_2 + H_2$	8.0×10^{13}	0.0	8.0×10^{13}	3.9×10^{2}	−3.8	−69.5	24
153	$C_2H_3^{\bullet} + CH_3^{\bullet} \rightarrow C_2H_2 + CH_4$	1.0×10^{13}	0.0	1.0×10^{13}	9.4×10^{2}	−10.4	−70.4	1
154	$C_2H_3^{\bullet} + CH_3^{\bullet} \rightarrow C_3H_6$	7.2×10^{13}	0.0	7.2×10^{13}	6.1×10^{-1}	−40.4	−102.4	25
155	$HCO^{\bullet} + Ar \rightarrow H^{\bullet} + CO + Ar$	2.5×10^{14}	16.9	2.8×10^{11}	1.1×10^{14}	25.2	17.7	11
156	$CH_3CO^{\bullet} + Ar \rightarrow CH_3^{\bullet} + CO + Ar$	1.2×10^{15}	12.5	8.0×10^{12}	4.4×10^{13}	30.9	14.3	11
157	$C_2H_5^{\bullet} \rightarrow C_2H_4 + H^{\bullet}$	3.6×10^{12}	37.2	1.1×10^{6}	2.1×10^{12}	24.9	38.3	12
158	$C_4H_3^{\bullet} \rightarrow C_4H_2 + H^{\bullet}$	1.0×10^{14}	40.0	1.0×10^{7}	3.0×10^{13}	24.2	38.6	26
159	$C_4H_4 \rightarrow C_4H_3^{\bullet} + H^{\bullet}$	2.0×10^{14}	103.0	2.0×10^{-4}	7.6×10^{12}	33.0	107.4	1
160	$C_4H_3^{\bullet} + CH_3^{\bullet} \rightarrow C_4H_2 + CH_4$	3.9×10^{11}	0.0	3.9×10^{11}	49	−10.0	−69.2	1
161	$C_4H_4 + CH_3^{\bullet} \rightarrow CH_4 + C_4H_3^{\bullet}$	3.0×10^{13}	14.0	1.1×10^{11}	1.7×10^{11}	−1.2	−0.3	1
162	$C_4H_3^{\bullet} + H^{\bullet} \rightarrow C_4H_2 + H_2$	8.1×10^{13}	0.0	8.1×10^{13}	5.3×10^{2}	−3.5	−68.3	1
163	$C_4H_4 + H^{\bullet} \rightarrow C_4H_3^{\bullet} + H_2$	3.0×10^{14}	12.0	2.4×10^{12}	2.0×10^{11}	5.3	0.5	1
164	$C_4H_4 + C_3H_3^{\bullet} \rightarrow p\text{-}C_3H_4 + C_4H_3^{\bullet}$	1.0×10^{13}	15.0	2.4×10^{10}	7.6×10^{12}	0.0	14.3	1
165	$C_4H_3^{\bullet} + C_2H_3^{\bullet} \rightarrow CH{\equiv}C{-}CH{=}CH{-}CH{=}CH^{\bullet} + H^{\bullet}$	5.0×10^{13}	15.0	1.2×10^{11}	6.3×10^{12}	−11.0	−3.9	1
166	$C_4H_3^{\bullet} + C_2H_3^{\bullet} \rightarrow C_4H_4 + C_2H_2$	5.0×10^{11}	0.0	5.0×10^{11}	29	−9.2	−70.0	1
167	$C_4H_3^{\bullet} + C_2H_3^{\bullet} \rightarrow C_4H_2 + C_2H_4$	5.0×10^{11}	0.0	5.0×10^{11}	8.4	−11.1	−75.5	1
168	$CH{\equiv}C{-}CH{=}CH{-}CH{=}CH^{\bullet} \rightarrow C_4H_3^{\bullet} + C_2H_2$	5.0×10^{14}	38.0	1.1×10^{8}	4.8×10^{12}	34.8	41.4	12
169	$C_3H_3^{\bullet} + C_3H_3^{\bullet} \rightarrow C_6H_6$	1.5×10^{13}	0.0	1.5×10^{13}	4.3×10^{-5}	−60.1	−146.8	1
170	$C_3H_6 + H^{\bullet} \rightarrow CH_3^{\bullet} + C_2H_4$	3.5×10^{14}	9.0	9.4×10^{12}	6.3×10^{9}	5.1	−11.7	1
171	$C_2H_4 + H^{\bullet} \rightarrow C_2H_3^{\bullet} + H_2$	5.4×10^{14}	14.9	1.4×10^{12}	5.3×10^{11}	7.7	7.3	24
172	$C_2H_4 + CH_3^{\bullet} \rightarrow C_2H_3^{\bullet} + CH_4$	$6.6T^{+3.70}$	9.5	4.2×10^{10}	3.1×10^{11}	1.1	6.4	24
173	$C_2H_4 + CH_3^{\bullet} \rightarrow nC_3H_7^{\bullet}$	3.3×10^{11}	7.7	1.5×10^{10}	5.8×10^{7}	−29.9	−22.5	24
174	$nC_3H_7^{\bullet} \rightarrow C_3H_6 + H^{\bullet}$	1.8×10^{14}	38.2	3.8×10^{7}	1.5×10^{13}	24.8	34.2	12
175	$C_2H_6 + H^{\bullet} \rightarrow C_2H_5^{\bullet} + H_2$	1.2×10^{14}	9.6	2.6×10^{12}	7.1×10^{9}	8.0	−4.6	12
176	$CH_3^{\bullet} + CH_3^{\bullet} \rightarrow C_2H_6$	$1.0 \times 10^{15}T^{-0.64}$	0.0	1.1×10^{13}	9.8	−40.3	−90.5	24
177	$C_2H_4 + C_3H_3^{\bullet} \rightarrow C_2H_3^{\bullet} + a\text{-}C_3H_4$	2.0×10^{12}	25.0	8.5×10^{7}	3.8×10^{11}	1.3	22.5	est
178	$C_2H_4 + C_3H_3^{\bullet} \rightarrow C_2H_3^{\bullet} + p\text{-}C_3H_4$	2.0×10^{12}	23.5	1.6×10^{8}	2.3×10^{11}	2.3	21.0	est
179	$C_3H_5^{\bullet} + H^{\bullet} \rightarrow a\text{-}C_3H_4 + H_2$	1.8×10^{13}	0.0	1.8×10^{13}	6.7×10^{5}	−4.0	−47.5	27
180	$C_3H_3O^{\bullet} \rightarrow CO + C_2H_3^{\bullet}$	5.0×10^{13}	25.0	2.1×10^{9}	1.1×10^{13}	28.1	27.7	est
181	$C_2H_6 + C_3H_5^{\bullet} \rightarrow C_2H_3^{\bullet} + C_3H_6$	$2.35 \times 10^{2}T^{+3.3}$	19.8	3.5	1.3×10^{12}	−7.1	57.4	27

[a] (Units are cm^3, mol^{-1}, s^{-1}, kcal/mol and cal/(k mol). Values Are Given at 1250 K). [b] est = estimated. [c] 1*: ref 1, modified.

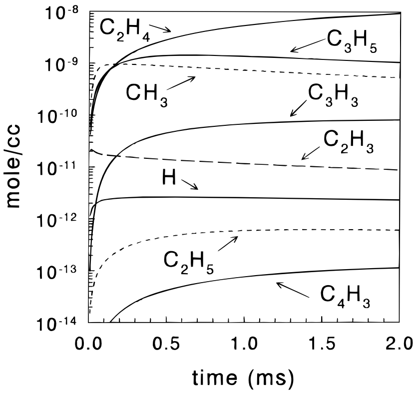

Figure 8. Radical profiles, calculated at 1250 K. The profile of C_2H_4 is also shown for comparison.

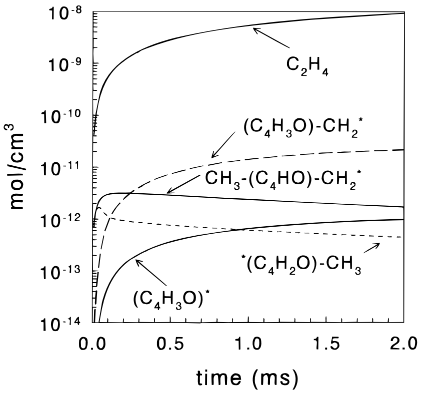

Figure 9. Radical profiles, calculated at 1250 K. The profile of C_2H_4 is also shown for comparison.

taken into account in view of the high concentration of the latter as a reactant, at least at the low temperature end of the study. The concentrations of $HCO^{\bullet}$, $C_2H_3^{\bullet}$, and $C_2H_5^{\bullet}$ as can be seen in Figure 8 are very small, and their abstraction reactions can be neglected. The concentration of all the free radicals are shown as a function of time in Figures 8−11. Since most of the abstraction reactions that appear in the reaction scheme had to be estimated, we had to assign values for the preexponential factors and activation energies for these constants. Preexponential factors ranged from approximately 5×10^{11} to 5×10^{14} $cm^3mol^{-1}s^{-1}$, going form large free radicals to $H^{\bullet}$. Activation energies ranged between 6 and 17 kcal/mol depending upon the size of the radical and the thermochemistry of the abstraction reactions.

It should be mentioned that many of the abstraction reactions have no influence on the overall decomposition rate of 2,5-dimethylfuran. Specific abstractions, however, affect the concentrations of several low-yield species. The concentrations of the latter, in most cases, are not very sensitive to the exact values of the abstraction rate constants. However, if they are removed from the reaction scheme, the concentrations of these species are affected. Thus the Arrhenius parameters of these estimates

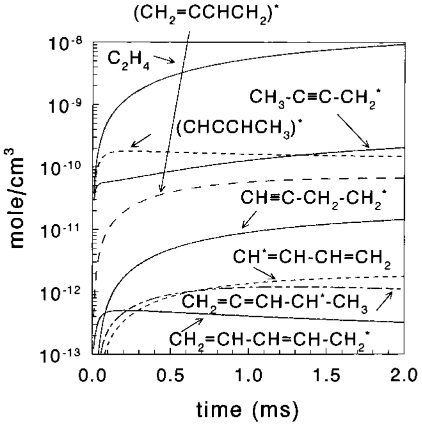

Figure 10. Radical profiles, calculated at 1250 K. The profile of C_2H_4 is also shown for comparison.

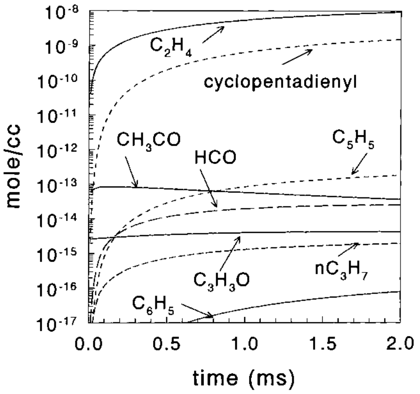

Figure 11. Radical profiles, calculated at 1250 K. The profile of C_2H_4 is also shown for comparison.

rate constants are approximate values and should not be considered as absolute values.

b. Recombinations. As in every scheme containing free radical reactions, there are recombinations in this scheme as well. Since the number of free radicals is rather large, and since we did not recover products having more than six carbon atoms, we have included recombinations of radicals having together no more than six carbon atoms. Also, free radicals with very low concentrations were not included. Preexponential factors for some of the recombinations were estimated. Recombination rates depend on the free radical sizes and vary from approximately 4×10^{11} for large species to 3×10^{13} for methyl groups.

c. Dissociative Attachments. This is one of the most important class of reactions involving free radicals. They replace highly endothermic unimolecular dissociations that require high activation energies by bimolecular reactions with relatively low activation energies. These class of reactions is very common, for example, in organic nitriles ($R-C\equiv N$).[8,9] The dissociations of such molecules to $R^\bullet + CN^\bullet$ are highly endothermic and thus have very high activation energies, whereas the dissociative attachment $R-C\equiv N + H^\bullet \rightarrow R^\bullet + HCN$ has a very low activation energy. These type of reactions are known in many systems and their importance is determined by the steady-state concentrations of hydrogen atoms. Dissociative attachments of the type 2,5-dimethylfuran + $H^\bullet \rightarrow CH_3CO^\bullet + C_4H_6$ and others are very important in the present system.

d. Unimolecular Decompositions of Unstable, Free Radical Intermediates. In the process H-atom or methyl group ejection from the molecule or in the process of ring cleavage, unstable intermediates are formed. They further decompose to smaller fragments. Several reactions which describe such processes are present in the reaction scheme. The decomposition of $CH_3(C_4H_2O)CH_2^\bullet$ or $CH_3(C_4H_2O)^\bullet$ to smaller fragments follow closely the decomposition pattern of 2,5-dimethylfuran and 2-methylfuran.[1] They are very important reactions in the scheme. Some of the rate parameters for this decomposition, for example, that of the reaction $CH_3CO^\bullet \rightarrow CH_3^\bullet + CO$ are known.[11] Others were estimated based on comparison with rates of similar stable fragment taking into account the endothermicity of the reaction.

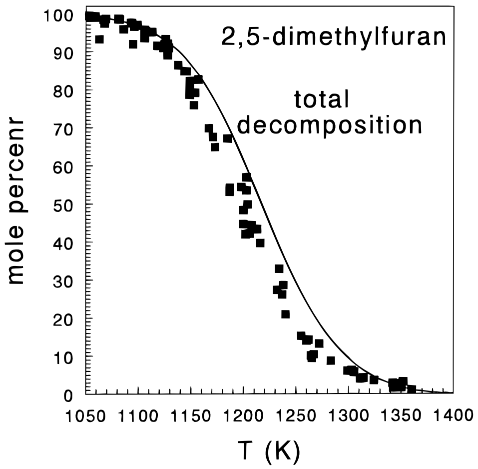

Figure 12. Experimental and calculated mole percent of 2,5-dimethylfuran, showing its total decomposition.

4. Comments on Specific Products. *a. C_5H_6.* As was demonstrated in Figure 7, two isomers of C_5H_6 are present among the reaction products. The larger peak was identified as cyclopentadiene and the much smaller one as 1,2,4-pentatriene. These two isomers are formed via two, completely different, routes.

Cyclopentadiene is formed via a 1,4-cyclization of $CH_2{=}CH{-}CH{=}CH{-}CH_2^\bullet$ together with a H-atom ejection: $CH_2{=}CH{-}CH{=}CH{-}CH_2^\bullet \rightarrow$ cyclopentadiene + H, where $CH_2{=}CH{-}CH{=}CH{-}CH_2^\bullet$ is formed by rearrangement of the decomposition products of the radical $CH_3(C_4H_2O)CH_2^\bullet$:

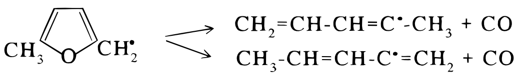

No matter whether the $-CH_3$ or the $-CH_2^\bullet$ group in $CH_3(C_4H_2O)CH_2^\bullet$ migrates in the process of CO elimination, the only free radical that can be formed is $CH_2{=}CH{-}CH{=}CH{-}CH_2^\bullet$.

$$CH_2{=}CH{-}CH{=}C^\bullet{-}CH_3 \rightarrow CH_2{=}CH{-}CH{=}CH{-}CH_2^\bullet \quad \text{(1,2-H-atom migration)}$$

$$CH_3{-}CH{=}CH{-}C^\bullet{=}CH_2 \rightarrow CH_2{=}CH{-}CH{=}CH{-}CH_2^\bullet \quad \text{(1,4-H-atom migration)}$$

Both 1,2- and 1,4-H-atom migration will lead to the production of the same species. No other radical that may finally lead to the formation of 1,2,4-pentatriene by H-atom ejection can thus be formed.

1,2,4-Pentatriene must be formed by another channel and the only possible channel is the one in which C_5H_8 and later the $CH_2{=}C{=}CH{-}CH^\bullet{-}CH_3$ radical are the precursors. Since the concentrations of the two C_5H_8 isomers are rather small, the concentration of 1,2,4-pentatriene is very small compared to

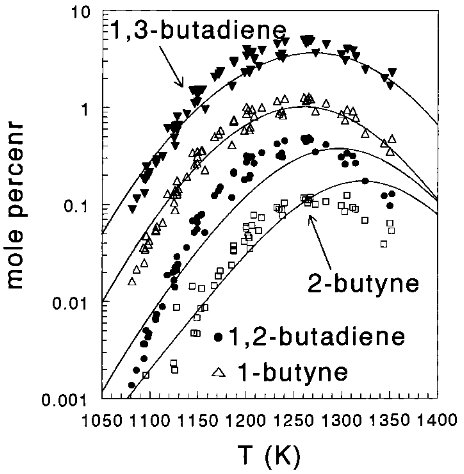

Figure 13. Experimental and calculated mole percent of the four isomers of C_4H_6.

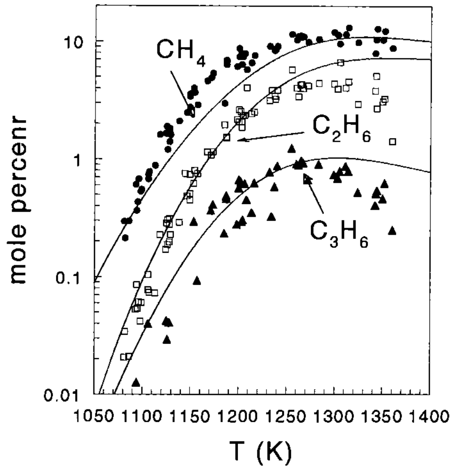

Figure 14. Experimental and calculated mole percent of methane and ethane and propylene.

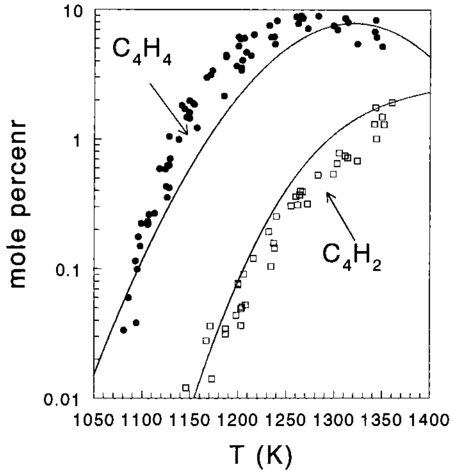

Figure 15. Experimental and calculated mole percent of C_4H_4 and C_4H_2.

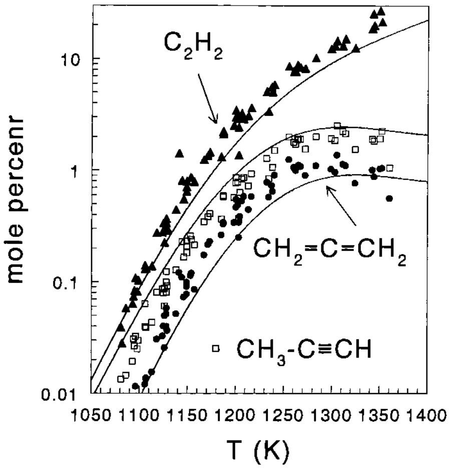

Figure 16. Experimental and calculated mole percent of allene, propyne, and acetylene.

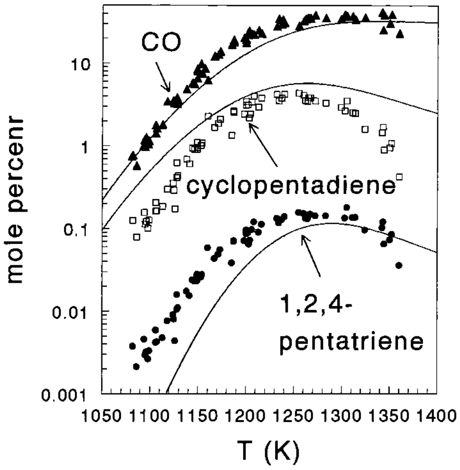

Figure 17. Experimental and calculated mole percent of carbon monoxide and the two isomers of C_5H_6.

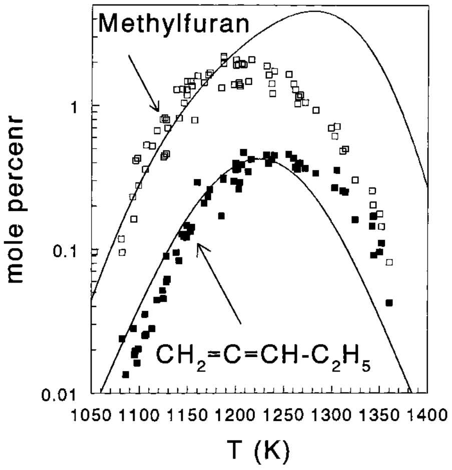

Figure 18. Experimental and calculated mole percent of 2-methylfuran and 1,2-pentadiene.

that of cyclopentadiene, as can be seen in Figure 7. The reaction sequence for the production of cyclopentadiene is thus 17, 40, and 126 (Table 3), and the major one of 1,2,4-pentatriene is 2, 121, and 125.

b. C_4H_6. Four isomers of C_4H_6, 1,2- and 1,3-butadiene, and 1- and 2-butyne, were found among the products formed as a result 2,5-dimethylfuran decomposition. Their distribution, shown in Figure 13, is very similar to what has been observed in the decomposition of 2-methylfuran, although the isomers' formation mechanism are very different. In 2-methylfuran they are formed by unimolecular cleavage of the ring, whereas in 2,5-dimethylfuran they are produced by processes which include free radicals. Among these processes are the unimolecular decomposition of 2,5-dimethylfuran to $CH_3CO^•$ and $C_4H_5^•$ followed by H-atom recombination with $C_4H_5^•$, and the dissociative attachments of H-atom to 2,5-dimethylfuran with the

TABLE 4: Sensitivity Spectrum at 1100/1300 K for Elimination of Reactions from the Kinetic Scheme. Percent Change in Yield for Reaction Elimination

reaction number	1,3-butadiene	1,2-butadiene	1-butyne	2-butyne	C_4H_4	C_4H_2	cyclopentadiene	1,2,4-pentatriene	1,3-pentadiene	1,2-pentadiene
1								−/−32	−99/−99	
2								−87/−36		−60/−39
3										−86/−
7	−19/−	−23/−15		−90/−20	−47/−19	−59/−28				
8	−20/−	−23/−28	−81/−37	−/−22		−34/−	−26/−			−21/−
9	−24/−	−24/−				−24/−			−/22	
10	−99/−77	63/−		20/−	−/−23					−/−23
12		−90/−								
13			−23/−							
14	65/33	63/38		20/42						
17	−66/−	−65/−		−21/−	−49/−	−43/−	−84/−47			−/23
18										37/−
19										37/−
21				−68/−						
22			−78/−37							
40	−78/−	−77/−		−22/−	434/51	460/71	−99/−95			−22/29
41					−56/−	−56/−				
56				−/−33						
64			−/47							
65		−/111		217/208	−40/−21	−46/−32				
66			−/23							
67										26/−
68	−/28				−/−21	−/−22		−/88		−/182
76				−/33						
77	−/24									−/−28
82			−/23							
110								−/−33		
114									−/25	
118								−/35		−/79
119										−59/34
121								−81/−44		
125								−90/−65		
126	−77/−17	−76/−		−24/−	−30/−	−70/−	−99/−99	−53/139	−/741	65/−
144	−21/−									
145										−94/−
151	−30/−	−30/−				−39/−	−25/−	−25/−		
156	−47/−	−47/−			−37/−42	−83/−50	−62/−	−64/−26		
157										−/45
158						−98/−97				
161						−97/−84				
176	58/−25	60/31		21/30	49/−	200/100	78/26	110/160	−/−41	−/44

reaction number	CO	CH_4	C_2H_4	C_2H_6	C_2H_2	C_3H_6	allene	propyne	methylfuran	C_6H_6
2										−60/−
3			−37/−22					−87/−33		−86/−26
4							−71/−			
7		−20/−		−35/−					−20/−	
8	−22/−	−21/−		−37/−					−21/−	−21/−
9	−21/−			−30/−	−93/−38	−77/−67	−15/−23		−25/−	
10			36/−				−/22	−/21	65/31	
14			37/31	−/−21					−99/−99	
15			−55/−29	22/−		−27/−				
17	−58/−	−98/−35	−37/−	20/24					−66/−	
18										37/−
19										37/−
20						−70/−				
38									−/22	
40	−23/−		−44/−			−22/−			−78/−	−22/−21
67										26/24
68							−/−21	−/−29		−/83
119										−59/−22
126	−46/−	−57/−	−43/−	−81/−		−39/−40	−/−64	−/−44	−78/−23	65/67
143								−/−32		−/−26
144							−21/−24			
145								−/27		−94/−64
146					−/−29					
148					−/−27	−/23	−/52	−/46		−/35
151	−20/−	−28/−		−49/−	−75/−25	159/146			−31/−	
154						−28/−64				
156	−65/−38	−74/−37	−27/−	−93/−64		−35/−23			−48/−	
158								−/−30		−/31
176	55/−	98/110	35/−	−99/−99		34/46			62/−	
181				−20/−	−80/−19	−34/−37				

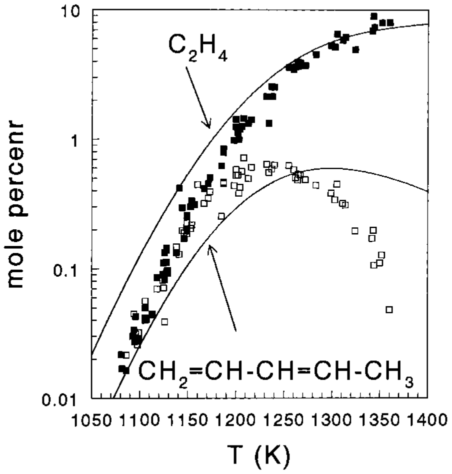

Figure 19. Experimental and calculated mole percent of ethylene and 1,3-pentadiene.

production of C_4H_6 and $CH_3CO^\bullet$. There are also isomerization reactions among the various C_4H_6[6] species and a number of competition reactions that can vary the distribution among them depending upon their rate constants.

c. C_4H_4 and C_4H_2. The yield of C_4H_4 among the decomposition products is relatively high. There are at least two major channels that are responsible for its production. The more important one is $CH_3(C_4H_2O)CH_2^\bullet \rightarrow CH_3CO^\bullet + C_4H_4$ but $C_4H_5^\bullet \rightarrow C_4H_4 + H^\bullet$ also contributes to the production of C_4H_4. If each one of these is removed from the reaction scheme, the yield of C_4H_4 goes down. All the reactions that are responsible for the production of $CH_3(C_4H_2O)CH_2^\bullet$ or $C_4H_5^\bullet$ have also a strong influence on the yield of C_4H_4. C_4H_2, on the other hand, whose yield is rather small, is formed by one reaction channel at the end of which stands the reaction $C_4H_3^\bullet \rightarrow C_4H_2 + H^\bullet$. If the latter is turned off, C_4H_2 disappears completely.

5. Reaction Scheme and Computer Modeling. To model the observed product distribution we have constructed a reaction scheme containing 50 species and 181 elementary reactions. The scheme is shown in Table 3. The rate constants listed in the Table are given as $k = A\exp(-E/RT)$ in units of cm^3, s^{-1}, kcal, and mol^{-1}. The Arrhenius parameters for the reactions in the scheme are either estimated as previously discussed or taken from various literature sources, mainly from the NIST-Kinetic Standard Reference Data Base 17.[12] The parameters for the reactions that were taken from the NIST-Kinetic Data Base are, in many cases, the best fit to a large number of entries. (In view of the very large number of citations involved in these cases, they are not detailed in the article.) The thermodynamic properties of the species involved were taken from various literature sources[13-16] or estimated using NIST-Standard Reference Data Base 25[13] (Structure and Properties program (SP)). We have performed sensitivity analysis with respect to variations (or rather uncertainties) in the ΔH^0_f of species whose thermodynamic properties were estimated or are not known accurately enough. Incorrect values of the thermodynamic functions result in erroneous values for the rate constants of the back reactions for a given value of the forward rate constant. In several sensitivity tests that were performed on the thermodynamic functions, we found that the results of the simulation were only slightly sensitive to variations in the estimated values.

Figure 12 shows the overall decomposition of 2,5-dimethylfuran. The squares are the experimental points and the line is the best fit to the calculated points taken at 25 K intervals. Figures 13−20 show comparisons between the experimentally measured yields and the calculated yields using the reaction scheme shown in Table 3. The agreement for most of the reaction products is satisfactory considering the large number of products obtained in this decomposition.

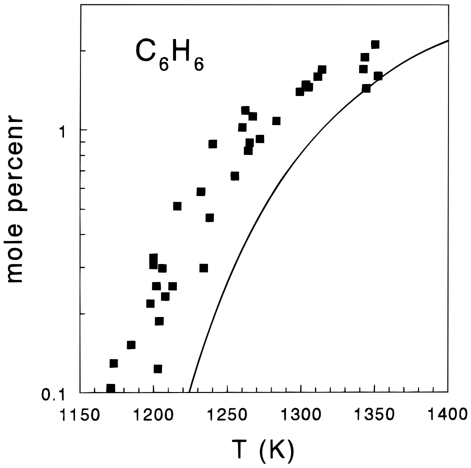

Figure 20. Experimental and calculated mole percent of benzene.

Table 4 gives the sensitivity of the products to elimination of specific reactions from the kinetic scheme, at 1100 and 1300 K, respectively. It gives the percent change in the yield of a particular product as a result of elimination of a given reaction from the scheme. The calculations were made for dwell times of 2 ms. Reactions that show an effect of less than 20% both at 1100 K and at 1300 K are not included in the table. A common feature to many reactions is the decreased sensitivity as the temperature increases. The number of channels that contribute to the formation of the products increase as the temperature increases and the effect of eliminating a single reaction diminishes.

Table 4 shows that only a relatively small number of elementary steps affect the product distribution in the sense that their elimination from the scheme affects the yield of at least one of the products. The majority of the elementary reactions that compose the scheme do not affect the distribution at all. They are left in the kinetic scheme for completeness and applicability beyond the temperature range of the present experiments. It should be mentioned, however, that the sensitivity analysis is done by removing a single reaction at a time and examining its effect. When a complete group of reactions is eliminated from the scheme there can be a strong effect on particular products although the elimination of only one step, as is shown in Table 4, does not affect anything.

Most of the sensitivities that appear in Table 4 are self-explanatory and enable one to follow the sequence of steps that lead to a particular product. Cyclopentadiene, for example, is formed by reaction 126 and is turned completely off when this reaction is removed. However, if either the main channel for the formation of $CH_3(C_4H_2O)CH_2^\bullet$ (reaction 17) or its decomposition to $CH_2{=}CH{-}CH{=}CH{-}CH_2^\bullet$ and CO (reaction 40) are removed from the scheme, the yield of cyclopentadiene drops almost to zero. This indicates that the formation sequence of cyclopentadiene is 17 → 40 → 126. Many similar examples can be found by examining of the sensitivity analysis data shown in Table 4.

References and Notes

(1) Lifshitz, A.; Tamburu, C.; Shashua, R. *J. Phys. Chem. A* **1997**, *101*, 1018.

(2) Grela, M. A.; Amorebieta, V. T.; Collusi, A. J. *J. Phys. Chem.* **1985**, *89*, 38.

(3) Lifshitz, A.; Moran, A.; Bidani, S. *Int. J. Chem. Kinet*. **1987**, *19*, 61.

(4) Tsang, W.; Lifshitz, A. *Int. J. Chem. Kinet.* **1998**. In press.

(5) Lifshitz, A.; Bidani, M.; Agranat, A.; Suslensky, A. *J. Phys. Chem.* **1987**, *91*, 6043.

(6) Hidaka, Y.; Higashihara, T.; Ninomiya, N.; Oshita, H.; Kawano, H. *J. Phys. Chem.* **1993**, *97*, 10977.

(7) Muller-Markgraf, W.; Troe, J. In *Proceedings of the 21st International Symposium on Combustion*; The Combustion Institute: Pittsburgh, PA, 1986; p 815.

(8) Lifshitz, A.; Tamburu, C. *Int. J. Chem. Kinet.* **1998**, *30*, 341.

(9) Lifshitz, A.; Cohen, Y.; Braun-Unkhoff, M.; Frank, P. In *Proceedings of the 26th International Symposium on Combustion*; The Combustion Institute: Pittsburgh, PA, 1996; p 659.

(10) Laskin, A.; Lifshitz, A. *J. Phys. Chem. A* **1997**, *101*, 7787.

(11) Warnatz, J. *Rate Coefficients in the C/H/O System Combustion Chemistry*; Gardiner, W. C., Jr., Ed.; Springer-Verlag: New York, 1984; p 197.

(12) Westly, F.; Herron, J. T.; Cvetanovic, R. J.; Hampson, R. F.; Mallard, W. G. *NIST- Chemical Kinetics Standard Reference Database 17*, Ver. 5.0; National Institute of Standards and Technology: Washington, DC.

(13) Stein, S. E.; Rukkers, J. M.; Brown, R. L. *NIST- Standard Reference Database* 25; National Institute of Standards and Technology; Washington, DC.

(14) Melius, K. *BAC-MP4 Heats of Formation*; Sandia National Laboratories: Livermore, CA, March, 1993.

(15) Pedley, J. B.; Taylor, R. D.; Kirby, S. P. *Thermochemical Data of Organic Compounds*; Chapman and Hall: London, 1986.

(16) Burcat, A.; McBride, B.; Rabinowitz, M. *Ideal Gas Thermodynamic Data for Compounds Used in Combustion*; T. A. E. 657 Report; Technion, Israel Institute of Technology; Haifa, Israel, 1997.

(17) Nguyen, T. T.; King, K. D. *Int. J. Chem. Kinet.* **1982**, *14*, 623.

(18) Kern, R.; D.; Zhang, Q.; Yao, J.; Jursic, B. S.; Tranter, R. S.; Greybill, M. A.; Kiefer, J. H. In *Proceedings of the 27th International Symposium on Combustion*. In press.

(19) Roy, K.; Frank, P.; Just, T. *Isr. J. Chem.* **1996**, *36*, 275.

(20) Dean, A. M. *J. Phys. Chem.* **1990**, *94*, 1432.

(21) Lifshitz, A.; Frenklach, M.; Burcat, A. *J. Phys. Chem.* **1975**, *79*, 1148.

(22) Hidaka, Y.; Nakamura, T.; Miyauchi, A.; Shiraishi, T.; Kawano, H. *Int. J. Chem. Kinet.* **1989**, *21*, 643.

(23) Benson, S. W. *Int. J. Chem. Kinet.* **1989**, *21*, 233.

(24) Tsang W.; Hampson, R. F. *Phys. Chem. Ref. Data* **1986**, *15*, 1087.

(25) Fahr, A.; Laufer, A.; Klein, R.; Braun, W. *J. Phys. Chem.* **1991**, *95*, 3218.

(26) Weissman, M.; Benson, S. W. *Int. J. Chem. Kinet.* **1984**, *16*, 307.

(27) Tsang, W. *J. Phys. Chem. Ref. Data* **1991**, *20*, 221.

(28) Dean, A. M.; Westmoreland, P. R. *Int. J. Chem. Kinet.* **1987**, *19*, 207.